

PREPARATION AND CHARACTERIZATION OF SEBS-CLAY NANOCOMPOSITES

by
MESUT ÜNAL

Submitted to the Graduate School of Engineering and Natural Sciences
in partial fulfillment of
the requirements for the degree of
Master of Science

Sabanci University
Summer 2004

© MESUT ÜNAL 2004

All Rights Reserved

TABLE OF CONTENTS

Acknowledgements.....	i
Abstract.....	ii
Özet.....	iv
List of Figures.....	vi
List of Tables.....	ix
Abbreviations.....	x

CHAPTER 1

1. INTRODUCTION.....	1
1.1. SEBS Overview	1
1.1.1. Structure	3
1.1.2. Synthesis and Commercial Production	4
1.2. Polymer-Clay Nanocomposites.....	6
1.2.1. Structure and properties of layered silicates.....	6
1.2.2. Structure and properties of organically modified layered silicates (OMLS).....	8
1.2.3. Types of nanocomposites	9
1.2.4. Techniques used for the characterization of Nanocomposites.....	11
1.2.5. Preparative methods and morphological study.....	13
1.2.5.1. Intercalation of polymer or pre-polymer from solution....	13
1.2.5.2. In situ intercalative polymerization method.....	16
1.2.5.3. Melt Intercalation.....	21
1.2.6. Nanocomposites Properties.....	27

1.2.6.1. Mechanical properties.....	27
1.2.6.1.1. Dynamic mechanical analysis.....	29
1.2.6.1.2. Tensile properties.....	29
1.2.6.2. Heat distortion temperature.....	31
1.2.6.3. Thermal Stability.....	32
1.2.6.4. Fire Retardent Properties.....	34
1.2.6.5. Gas Barrier Properties.....	35
1.2.6.6. Optical Transparency.....	35

CHAPTER 2

2. EXPERIMENT.....	36
2.1. Materials.....	36
2.1.1. Surfactants and clay.....	36
2.1.2. SEBS, Styrene, Initiator, and others.....	37
2.2. Experimental Procedure.....	38
2.2.1. Clay Treatment.....	38
2.2.1.1. Quaternization of water soluble azo-initiator (V-50).....	38
2.2.1.2. Na ⁺ -MMT Treatment and characterization.....	38
2.2.2. Nanocomposite preparation and characterization.....	40

CHAPTER 3

3. RESULTS AND DISCUSSION.....	42
3.1. Novel idea for PCN preparation.....	42
3.2. Clay treatment.....	44
3.3. Nanocomposites and their properties.....	49

CHAPTER 4

4. CONCLUSIONS.....	55
REFERENCES.....	58

ACKNOWLEDGEMENTS

First of all, I would like to thank, my family for their continuous support, and trust.

I would like to thank my advisor, Dr. Yusuf Ziya Menceloglu, for his support, and creative attitude. He has guided me through my travel from University to Industry with his valuable advices. I have a new vision for future after two years. It was a pleasure to study under his supervision.

I am glad to have friends like Çınar Öncel, Karahan Bulut, Gizem Boyacioglu and Suzan Mutlu and I also thank to all my professors for their contribution.

I am proud of Turkish Companies trying to help the development of academia; Enplast A.S., Tekpar A.S., and Bensean A.S.

All my work is dedicated to the memory of my father who passed away a year ago following a sudden illness.

ABSTRACT

In this study, SEBS (styrene-*b*-ethylene-*b*-butylene-styrene) clay nanocomposites were synthesized with easy-to-find, cheap ingredients and using convenient, efficient and commercially viable methods. In particular, a combined melt intercalation method and *in-situ* intercalative polymerization method was implemented to produce nanocomposites. The underlying strategy of this approach was to treat clays with appropriately chosen surfactants, namely, those that possessed the ability to intercalate the basal spacings of the clay. An added subtlety of this study was the incorporation of an engineered polymerization initiator in the nanocomposite preparation, which behaved as an effective surfactant and permitted the uniform initiation of polymerization from even within basal spacings as opposed to being restricted to the clay surface.

In the first part of this study, the optimum surfactant for a given reaction condition was determined to be Tequart DSM (N-N dialkyl dimethyl ammonium chloride). Basal spacings noted via WAXD analysis showed that Na-MMT treated with Tequart DSM had reached values of up to 1.9 nm, which exceeded the value of 1.2 nm that is typical of pristine clay. Notably, Tequart DSM delaminated more effectively than Cloisite 15 A, a commercial organoclay (1.38 nm). BTC 1218-50 (Alkyl dimethyl benzyl ammonium chloride) was also successful in view that the value noted was about 1.4 nm. Subsequently, an appropriate surfactant-initiator was envisaged and afforded by methylating the water-soluble radical initiator, V-50 (2,2'-Azobis-2-methyl propionamide). Methylation was confirmed by the appearance of additional resonances on the ¹H-NMR spectrum and by the shift of the melting curve from 173.9 °C to 119.5 °C on the DSC thermogram. While NMR analysis indicated that an average of four methyl groups had been attached to the native structure, DSC thermograms implied high product purity in view that the new melting endotherm was sharp. By applying this *in-situ* intercalative polymerization strategy to the best surfactant and initiator pair, a Styrene-clay nanocomposite masterbatch was realized. Clay, modified using an equimolar ratio of Tequart DSM and methylated V-50, displayed the greatest interlayer distance of 2.35 nm when characterized using WAXD. While this

sample (MC1) gave the best results, the interlayer spacings of other preparations were also notable: Tequart DSM-native V-50 (MC6) gave 2.02 nm, BTC 1218-50-treated V-50 (MC4) gave 1.07 nm, and BTC 1218-50-untreated V-50 (MC2) gave 1.07 nm.

In the final part of the thesis, several approaches for the preparation of nanocomposites were tested on a standard unfilled SEBS grade material. Each attempt was melt-mixed with SEBS and compression molded plaques were tested. Thermogravimetric analyses were carried out primarily to verify the anticipated clay content in each of the blends. SEM images in agreement with WAXD data proved that the nanocomposite produced was in fact intercalative. Tensile testing of polymer blends containing 5wt% intercalated clays displayed greater elongation values in all of the nanocomposites when compared with unfilled SEBS. For example, the maleic anhydride grafted SEBS (SEBS-MA) sample had the highest elongation value (642,87%). The sample representing our strategy, namely, a MC1 masterbatch (MC1-MB) containing nanocomposite, was more easily elongated than MC1 5% clay samples, even though it contained more styrene. Another interesting finding was the decreased tensile strength of the nanocomposites when compared to unfilled SEBS. Lastly, as the clay content was increased, the maximum elongation values were found to decrease.

To summarize, the combined melt intercalation method and in-situ intercalative polymerization method did indeed afford nanocomposites with altered properties. Compatibilization through masterbatch preparation or SEBS-MA incorporation consistently improved maximum elongation values. The masterbatch technique also improved the tensile strength of nanocomposites, the reason being apparently related to the extra styrene content in matrix. It follows to reason that the continued development of such an intercalative strategy can greatly improve the compatibility and properties of a wide range of composite materials.

ÖZET

Bu çalışma nispeten ekonomik, kimyasal yüzey aktif kimyasallarla, daha verimli ve kolay ama endüstriyel anlamda uygulama sansi en yüksek ve üstün özelliklere sahip SEBS (stiren-b-etilen-b-bütilen-b-stiren)-kil (sodium montmorillonit) nanokompozitleri oluşturmayı amaçlamaktadır. Eriyik interkalasyon ve yerinde interkalatif polimerizasyon metodu birleştirilerek alternatif bir metod denenmiştir. Arastırma kil yüzeyinin ve tabakalar arası boşluğunun verimli bir biçimde modifiye edilip, uygun metoduyla nanokompozit sentezleme metodu bulmaya odaklanmıştır. Bu çalışmada yenilik oluşturan düşünce yüzey aktif malzemeler gibi davranan polimerizasyon başlatıcılarının nanokompozit hazırlama tekniklerine dahil edilmesidir. Interkalatif polimerizasyon, verimli yüzey aktif madde-baslatıcı kombinasyonu varlığında kil modifikasyonundan sonra, bu ürünün masterbatch-nanokompozit (stiren-sodyum montmorillonite) haline dönüştürülmesinde kullanılmıştır. Daha sonra bu SEBS ile daha uyumlu bir yapı oluşturacağına inandığımız masterbatch dolgunuz SEBS kompozit ile eriyik halde karıştırılmıştır. Oluşan nanokompozitin özellikleri diğer tekniklerle hazırlanan örneklerle karşılaştırılmıştır.

Baslatıcı olarak kullanılan suda çözünen azo-baslatıcı 2,2'-Azobis(2-metilpropionamid) (V-50) kuarternize edilmiş ve reaksiyonun gerçekleştiği DSC ve ¹H-NMR ile teyid edilmiştir. DSC termografları modifiye edilmemiş baslatıcıya ait 173.9 °C'deki erime noktasının 119.5 °C'ye düştüğünü göstermiştir.

Daha sonra xisini difraktometre analizi esasına göre en uygun yüzeyaktif madde kombinasyonu belirlenmiştir. Kil tabakaları arasındaki mesafe Bragg Kanunundan faydalanarak denenilen bütün yüzey aktif maddeler için hesaplanmıştır. Sodyum montmorillonit'teki bu mesafe Tequart DSM (N-N dialkil dimetil amonyum klorit) ile modifiye edilen kilde, ilk hali olan 1.2 nm'den 1.9 nm'ye çıkmıştır. Bu değer BTC 1218-50

(Alkil dimetil benzil ammonyum klorit) ile deney tekrarlandığında 1.4 nm civarında seyretmiş, ticari olarak üretilmiş Cloisite 15A'da ise 1.38 olarak hesaplanmıştır.

Molar esitlikle hazırlanmış Tequart DSM-modifiye edilmiş V-50 (MC1) kombinasyonunda ise bu rakam 2.35 nm'dir. Diğer kombinasyonların iyon değiştirme tekniği ile kil tabakalarını birbirinden uzaklaştırabilme değerleri şöyle özetlenebilir: Tequart DSM- V-50 (MC6), 2.02 nm; BTC 1218-50-modifiye edilmiş V-50 (MC4), 1.07 nm, ve BTC 1218-50-V-50 (MC2), 1.07 nm.

Çalışmanın son bölümü SEBS ürününden ve MC1 adlı kilden çeşitli metodlarla nanokompozit sentezlenmesini kapsamaktadır. Her deney sonucu oluşan numuneler kompresyon kalıplama yöntemiyle oluşturulup karşılaştırma amaçlı testlere tabii tutulmuştur. Termogravimetrik analiz yöntemiyle numunelerin ihtiva ettikleri kil numuneleri teyid edilmiştir. Çekme-kopma testi sonucunda bütün nanokompozitlerde kopmada uzama değeri dolgunuz ürüne göre artmış kopma mukavemeti ise azalmıştır. Malzemenin içindeki kil miktarı arttıkça kopmada uzama değeri düşmüştür. Maleik anhidrit graft edilmiş SEBS (SEBS-MA) ihtiva eden numune en yüksek uzama değerine ulaşmıştır (642,87%). Bizim yeniliğimizi temsil eden MC1 masterbatch (%25 kil) (MC1-MB) nanokompoziti (% 5 kil), yapısında daha fazla stiren polimeri içermesine rağmen MC1'in olduğu gibi kullanıldığı %5 kil ihtiva eden numune karşılaştırıldığında daha fazla uzadı. Masterbatch hazırlama yoluyla veya maleik anhidrit kullanılarak arttırılan kompetibilizasyon kopmada uzama değerlerini yükseltmiştir. Masterbatch tekniği yapıya eklediği ekstra polistiren yüzünden aynı zamanda kopma mukavemetini yükseltmiştir. SEM imajları ise x-isini difraktometresi ölçümleriyle aynı doğrultuda oluşan nanokompozitin interkalatif olduğunu ispatlamış aynı zamanda kil parçacıklarının polimer matriksine homojen dağılımını göstermiştir.

LIST of FIGURES

Figure 1.1.	Comparison of TPE fabrication to that of thermoset rubber	2
Figure 1.2.	Demonstration of SEBS structure.....	4
Figure 1.3.	Synthesis of SEBS step 1.....	4
Figure 1.4.	Synthesis of SEBS step 2.....	4
Figure 1.5.	Synthesis of SEBS step 3.....	5
Figure 1.6.	Hydrogenation of the isomers.....	5
Figure 1.7.	Structure of 2:1 Phyllosilicates	7
Figure 1.8.	Arrangements of Alkylammonium ions in mica-type layered silicates with different layer charges.....	9
Figure 1.9.	Schematically illustration of three different types of thermodynamically stable PCN	9
Figure 1.10.	WAXD patterns and TEM images of three different types of PCN	11
Figure 1.11.	Schematic illustration of nanocomposite synthesis.....	14
Figure 1.12.	WAXD patterns of (a) four different organo clays and (b)corresponding nanocomposites	15
Figure 1.13.	WAXD patterns of ? amino acid (COOH-(CH ₂) _{n-1} -NH ₂) modified Na ⁺ -MMT.....	16
Figure 1.14.	Swelling behaviour of ? -amino acid modified MMT by ε-caprolactam.	16
Figure 1.15.	15 WAXD patterns of various monomer/OMLS and corresponding polymer nanocomposites.....	19
Figure 1.16.	TEM images of nanocomposites	19
Figure 1.17.	Schematic illustration of the intercalation process between a polymer melt and OMLS.....	21
Figure 1.18.	Representative WAXD of PS35/OMLS hybrid heated to 165 °C for various times.....	22

Figure 1.19.	Schematic representation of the dispersion process of OMLS in the PP matrix with the aid of PP-MA	24
Figure 1.20.	Surfactants used: N-N dialkyl dimethyl ammonium chloride (left), Alkyl dimethyl benzyl ammonium chloride (right).....	25
Figure 1.21.	Chemical Structure of Azo-initiator 2,2'-Azobis(2-methyl propionamide)..	26
Figure 1.22.	Temperature dependence of G', G'', and tan d for PP-MA matrix and various PPCNs.....	28
Figure 1.23.	Tensile characterization of the PP/fMMT nanocomposites.....	29
Figure 1.24.	TGA curves for polystyrene, PS and the nano composites.....	30
Figure 1.25.	Formation of tortuous path in PLS nanocomposites.....	32
Figure 1.26.	UV-vis transmittance spectra of PVA/MMT nanocomposites containing 4 and 10 wt.% MMT	37
Figure 2.1.	Clay treatment procedure	37
Figure 3.1.	¹ H-NMR spectra of water soluble azo-initiator before (left) and after (right) quaternization with dimethylsulfide.....	42
Figure 3.2.	DSC thermogram of water soluble azo-initiator before (left) and after (right) quaternization with dimethylsulfide.....	45
Figure 3.3.	Comparison of WAXD patterns of treated clays and commercial grades	43
Figure 3.4.	Thermogravimetric Analysis of Na ⁺ -MMT treated with two surfactants...	45
Figure 3.5.	WAXD patterns of surfactant-initiator pairs.....	46
Figure 3.6.	Thermogravimetric Analysis of surfactant-initiator pairs.....	47
Figure 3.7.	SEM image of MC1-polystyrene masterbatch.....	48
Figure 3.8.	WAXD patterns of various melt blends.....	48
Figure 3.9.	Thermogravimetric analysis of melt blends.....	49

Fig.3.10 SEM image of unfilled SEBS (left) and MC1-MB nanocomposite.....	51
Fig. 3.11 SEM images of MC1-MB nanocomposite at higher magnification.....	52

LIST of TABLES

Table 1.1.	Chemical Formula and Characteristics of commonly used Clays.....	7
Table 1.2.	Summary of melt intercalation of M2C18 and F2C18 with styrene derivative polymers.....	23
Table 1.3.	HDT of PP/MMT nanocomposites and the respective unfilled PP.....	30
Table 1.4.	Cone calorimeter data of various polymers and their nanocomposites with OMLS.....	31
Table 2.1.	Table of clay modifier contents.....	37
Table 3.1.	Mechanical properties of nanocomposites.....	50

ABBREVIATIONS

1,1- bis, t-butyl peroxy

2,2'-AZOBIS, 2-methyl propionamide

2C18, dioctadecyldimethylammonium

BTC 1218-50, Alkyl dimethyl benzyl ammonium chloride

C18, octadecylammonium

CEC, cation exchange capacity

CL, ϵ -caprolactone

DSC, differential scanning calorimetry

DMA, dynamic mechanical analysis

DMF, dimethylformamide

EPDM, ethylene propylene diene methylene linkage rubber

EB, ethylene and butylene

F, fluorohectorite

FR, flame retardants

G' , storage modulus

G'' , loss modulus

G''/G' , $\tan \delta$; the ratio (dikkat)

HDPE, high-density polyethylene

HMW, high molecular weight

HDT, heat distortion temperature

HRR, heat release rate

MA, maleic anhydrite

MB, masterbatch

MC2, BTC 1218-50-untreated V-50

MC4, BTC 1218-50-treated V-50

MC1, tequart DSM-treated V-50

MC6, tequart DSM-untreated V-50

MC, modified clay

MMA, methyl methacrylate

MPA, mega pascal

MMT, montmorillonite

N6, nylon-6

NA+-MMT, na-montmorillonite

NMR, nuclear magnetic resonance

OC, organoclays

OMLS, organically modified layered silicate

PCN, polymer-clay nanocomposites

PEO, polyethylene oxide

PVA, poly(vinyl alcohol)

PLS, polymer/layered silicate

PVP, poly(N-vinyl pyrrolidone)

PCL, poly(ϵ -caprolactone)

PLA, polylactide

PDMS, poly(dimethylsiloxane)

PS, polystyrene

PMMA, poly(methyl methacrylate)

PP, polypropylene

PP-MA, maleic anhydride grafted polypropylene;

PPCN, pp/clay nanocomposites

QA+, quaternary ammonium cation

QC18, octadecyltrimethylammonium

SEBS, styrene-block-ethylenebutylene-block-styrene

SBR, 1,3 styrene-butadiene copolymer

SBS, poly(styrene-block-butadiene-block-styrene)

SIS, poly(styrene-block-isoprene-block-styrene)

STN, methyltrioctylammonium modified smectite

SPN, diethylmethylammonium modified smectite

S, styrene

SAP, saponite

SEBS-MA, maleic anhydride grafted sebs

TPE, thermoplastic elastomers

TEQUART DSM, n-n dialkyl dimethyl ammonium chloride

TEM, transmission electron microscopy

TGA, thermogravimetric analysis

THF, tetrahydrofuran

WAXD, wide angle X-ray diffraction

PREPARATION AND CHARACTERIZATION OF SEBS-CLAY NANOCOMPOSITES

by
MESUT ÜNAL

Submitted to the Graduate School of Engineering and Natural Sciences
in partial fulfillment of
the requirements for the degree of
Master of Science

Sabanci University
Summer 2004

© MESUT ÜNAL 2004

All Rights Reserved

TABLE OF CONTENTS

Acknowledgements.....	i
Abstract.....	ii
Özet.....	iv
List of Figures.....	vi
List of Tables.....	ix
Abbreviations.....	x

CHAPTER 1

1. INTRODUCTION.....	1
1.1. SEBS Overview	1
1.1.1. Structure	3
1.1.2. Synthesis and Commercial Production	4
1.2. Polymer-Clay Nanocomposites.....	6
1.2.1. Structure and properties of layered silicates.....	6
1.2.2. Structure and properties of organically modified layered silicates (OMLS).....	8
1.2.3. Types of nanocomposites	9
1.2.4. Techniques used for the characterization of Nanocomposites.....	11
1.2.5. Preparative methods and morphological study.....	13
1.2.5.1. Intercalation of polymer or pre-polymer from solution....	13
1.2.5.2. In situ intercalative polymerization method.....	16
1.2.5.3. Melt Intercalation.....	21
1.2.6. Nanocomposites Properties.....	27

1.2.6.1. Mechanical properties.....	27
1.2.6.1.1. Dynamic mechanical analysis.....	29
1.2.6.1.2. Tensile properties.....	29
1.2.6.2. Heat distortion temperature.....	31
1.2.6.3. Thermal Stability.....	32
1.2.6.4. Fire Retardent Properties.....	34
1.2.6.5. Gas Barrier Properties.....	35
1.2.6.6. Optical Transparency.....	35

CHAPTER 2

2. EXPERIMENT.....	36
2.1. Materials.....	36
2.1.1. Surfactants and clay.....	36
2.1.2. SEBS, Styrene, Initiator, and others.....	37
2.2. Experimental Procedure.....	38
2.2.1. Clay Treatment.....	38
2.2.1.1. Quaternization of water soluble azo-initiator (V-50).....	38
2.2.1.2. Na ⁺ -MMT Treatment and characterization.....	38
2.2.2. Nanocomposite preparation and characterization.....	40

CHAPTER 3

3. RESULTS AND DISCUSSION.....	42
3.1. Novel idea for PCN preparation.....	42
3.2. Clay treatment.....	44
3.3. Nanocomposites and their properties.....	49

CHAPTER 4

4. CONCLUSIONS.....	55
REFERENCES.....	58

ACKNOWLEDGEMENTS

First of all, I would like to thank, my family for their continuous support, and trust.

I would like to thank my advisor, Dr. Yusuf Ziya Menciloglu, for his support, and creative attitude. He has guided me through my travel from University to Industry with his valuable advices. I have a new vision for future after two years. It was a pleasure to study under his supervision.

I am glad to have friends like Çinar Öncel, Karahan Bulut, Gizem Boyacioglu and Suzan Mutlu and I also thank to all my professors for their contribution.

I am proud of Turkish Companies trying to help the development of academia; Enplast A.S., Tekpar A.S., and Bensean A.S.

All my work is dedicated to the memory of my father who passed away a year ago following a sudden illness.

ABSTRACT

In this study, SEBS (styrene-*b*-ethylene-*b*-butylene-styrene) clay nanocomposites were synthesized with easy-to-find, cheap ingredients and using convenient, efficient and commercially viable methods. In particular, a combined melt intercalation method and *in-situ* intercalative polymerization method was implemented to produce nanocomposites. The underlying strategy of this approach was to treat clays with appropriately chosen surfactants, namely, those that possessed the ability to intercalate the basal spacings of the clay. An added subtlety of this study was the incorporation of an engineered polymerization initiator in the nanocomposite preparation, which behaved as an effective surfactant and permitted the uniform initiation of polymerization from even within basal spacings as opposed to being restricted to the clay surface.

In the first part of this study, the optimum surfactant for a given reaction condition was determined to be Tequart DSM (N-N dialkyl dimethyl ammonium chloride). Basal spacings noted via WAXD analysis showed that Na-MMT treated with Tequart DSM had reached values of up to 1.9 nm, which exceeded the value of 1.2 nm that is typical of pristine clay. Notably, Tequart DSM delaminated more effectively than Cloisite 15 A, a commercial organoclay (1.38 nm). BTC 1218-50 (Alkyl dimethyl benzyl ammonium chloride) was also successful in view that the value noted was about 1.4 nm. Subsequently, an appropriate surfactant-initiator was envisaged and afforded by methylating the water-soluble radical initiator, V-50 (2,2'-Azobis-2-methyl propionamide). Methylation was confirmed by the appearance of additional resonances on the ¹H-NMR spectrum and by the shift of the melting curve from 173.9 °C to 119.5 °C on the DSC thermogram. While NMR analysis indicated that an average of four methyl groups had been attached to the native structure, DSC thermograms implied high product purity in view that the new melting endotherm was sharp. By applying this *in-situ* intercalative polymerization strategy to the best surfactant and initiator pair, a Styrene-clay nanocomposite masterbatch was realized. Clay, modified using an equimolar ratio of Tequart DSM and methylated V-50, displayed the greatest interlayer distance of 2.35 nm when characterized using WAXD. While this

sample (MC1) gave the best results, the interlayer spacings of other preparations were also notable: Tequart DSM-native V-50 (MC6) gave 2.02 nm, BTC 1218-50-treated V-50 (MC4) gave 1.07 nm, and BTC 1218-50-untreated V-50 (MC2) gave 1.07 nm.

In the final part of the thesis, several approaches for the preparation of nanocomposites were tested on a standard unfilled SEBS grade material. Each attempt was melt-mixed with SEBS and compression molded plaques were tested. Thermogravimetric analyses were carried out primarily to verify the anticipated clay content in each of the blends. SEM images in agreement with WAXD data proved that the nanocomposite produced was in fact intercalative. Tensile testing of polymer blends containing 5wt% intercalated clays displayed greater elongation values in all of the nanocomposites when compared with unfilled SEBS. For example, the maleic anhydride grafted SEBS (SEBS-MA) sample had the highest elongation value (642,87%). The sample representing our strategy, namely, a MC1 masterbatch (MC1-MB) containing nanocomposite, was more easily elongated than MC1 5% clay samples, even though it contained more styrene. Another interesting finding was the decreased tensile strength of the nanocomposites when compared to unfilled SEBS. Lastly, as the clay content was increased, the maximum elongation values were found to decrease.

To summarize, the combined melt intercalation method and in-situ intercalative polymerization method did indeed afford nanocomposites with altered properties. Compatibilization through masterbatch preparation or SEBS-MA incorporation consistently improved maximum elongation values. The masterbatch technique also improved the tensile strength of nanocomposites, the reason being apparently related to the extra styrene content in matrix. It follows to reason that the continued development of such an intercalative strategy can greatly improve the compatibility and properties of a wide range of composite materials.

ÖZET

Bu çalışma nispeten ekonomik, kimyasal yüzey aktif kimyasallarla, daha verimli ve kolay ama endüstriyel anlamda uygulama sansi en yüksek ve üstün özelliklere sahip SEBS (stiren-b-etilen-b-bütilen-b-stiren)-kil (sodium montmorillonit) nanokompozitleri oluşturmayı amaçlamaktadır. Eriyik interkalasyon ve yerinde interkalatif polimerizasyon metodu birleştirilerek alternatif bir metod denenmiştir. Arastırma kil yüzeyinin ve tabakalar arası boşluğunun verimli bir biçimde modifiye edilip, uygun metodu nanokompozit sentezleme metodu bulmaya odaklanmıştır. Bu çalışmada yenilik oluşturan düşünce yüzey aktif malzemeler gibi davranan polimerizasyon başlatıcılarının nanokompozit hazırlama tekniklerine dahil edilmesidir. Interkalatif polimerizasyon, verimli yüzey aktif madde-baslatıcı kombinasyonu varlığında kil modifikasyonundan sonra, bu ürünün masterbatch-nanokompozit (stiren-sodyum montmorillonite) haline dönüştürülmesinde kullanılmıştır. Daha sonra bu SEBS ile daha uyumlu bir yapı oluşturacağına inandığımız masterbatch dolgunuz SEBS kompozit ile eriyik halde karıştırılmıştır. Oluşan nanokompozitin özellikleri diğer tekniklerle hazırlanan numunelerle karşılaştırılmıştır.

Baslatıcı olarak kullanılan suda çözünen azo-baslatıcı 2,2'-Azobis(2-metilpropionamid) (V-50) kuarternize edilmiş ve reaksiyonun gerçekleştiği DSC ve ¹H-NMR ile teyid edilmiştir. DSC termografları modifiye edilmemiş baslatıcıya ait 173.9 °C'deki erime noktasının 119.5 °C'ye düştüğünü göstermiştir.

Daha sonra xisini difraktometre analizi esasına göre en uygun yüzeyaktif madde kombinasyonu belirlenmiştir. Kil tabakaları arasındaki mesafe Bragg Kanunundan faydalanarak denen bütün yüzey aktif maddeler için hesaplanmıştır. Sodyum montmorillonit'teki bu mesafe Tequart DSM (N-N dialkil dimetil amonyum klorit) ile modifiye edilen kilde, ilk hali olan 1.2 nm'den 1.9 nm'ye çıkmıştır. Bu değer BTC 1218-50

(Alkil dimetil benzil ammonyum klorit) ile deney tekrarlandığında 1.4 nm civarında seyretmiş, ticari olarak üretilmiş Cloisite 15A'da ise 1.38 olarak hesaplanmıştır.

Molar esitlikle hazırlanmış Tequart DSM-modifiye edilmiş V-50 (MC1) kombinasyonunda ise bu rakam 2.35 nm'dir. Diğer kombinasyonların iyon değiştirme tekniği ile kil tabakalarını birbirinden uzaklaştırabilme değerleri şöyle özetlenebilir: Tequart DSM- V-50 (MC6), 2.02 nm; BTC 1218-50-modifiye edilmiş V-50 (MC4), 1.07 nm, ve BTC 1218-50-V-50 (MC2), 1.07 nm.

Çalışmanın son bölümü SEBS ürününden ve MC1 adlı kilden çeşitli metodlarla nanokompozit sentezlenmesini kapsamaktadır. Her deney sonucu oluşan numuneler kompresyon kalıplama yöntemiyle oluşturulup karşılaştırma amaçlı testlere tabii tutulmuştur. Termogravimetrik analiz yöntemiyle numunelerin ihtiva ettikleri kil numuneleri teyid edilmiştir. Çekme-kopma testi sonucunda bütün nanokompozitlerde kopmada uzama değeri dolgunuz ürüne göre artmış kopma mukavemeti ise azalmıştır. Malzemenin içindeki kil miktarı arttıkça kopmada uzama değeri düşmüştür. Maleik anhidrit graft edilmiş SEBS (SEBS-MA) ihtiva eden numune en yüksek uzama değerine ulaşmıştır (642,87%). Bizim yeniliğimizi temsil eden MC1 masterbatch (%25 kil) (MC1-MB) nanokompoziti (% 5 kil), yapısında daha fazla stiren polimeri içermesine rağmen MC1'in olduğu gibi kullanıldığı %5 kil ihtiva eden numune karşılaştırıldığında daha fazla uzadı. Masterbatch hazırlama yoluyla veya maleik anhidrit kullanılarak arttırılan kompetibilizasyon kopmada uzama değerlerini yükseltmiştir. Masterbatch tekniği yapıya eklediği ekstra polistiren yüzünden aynı zamanda kopma mukavemetini yükseltmiştir. SEM imajları ise x-isini difraktometresi ölçümleriyle aynı doğrultuda oluşan nanokompozitin interkalatif olduğunu ispatlamış aynı zamanda kil parçacıklarının polimer matriksine homojen dağılımını göstermiştir.

LIST of FIGURES

Figure 1.1.	Comparison of TPE fabrication to that of thermoset rubber	2
Figure 1.2.	Demonstration of SEBS structure.....	4
Figure 1.3.	Synthesis of SEBS step 1.....	4
Figure 1.4.	Synthesis of SEBS step 2.....	4
Figure 1.5.	Synthesis of SEBS step 3.....	5
Figure 1.6.	Hydrogenation of the isomers.....	5
Figure 1.7.	Structure of 2:1 Phyllosilicates	7
Figure 1.8.	Arrangements of Alkylammonium ions in mica-type layered silicates with different layer charges.....	9
Figure 1.9.	Schematically illustration of three different types of thermodynamically stable PCN	9
Figure 1.10.	WAXD patterns and TEM images of three different types of PCN	11
Figure 1.11.	Schematic illustration of nanocomposite synthesis.....	14
Figure 1.12.	WAXD patterns of (a) four different organo clays and (b)corresponding nanocomposites	15
Figure 1.13.	WAXD patterns of ? amino acid (COOH-(CH ₂) _{n-1} -NH ₂) modified Na ⁺ -MMT.....	16
Figure 1.14.	Swelling behaviour of ? -amino acid modified MMT by ε-caprolactam.	16
Figure 1.15.	15 WAXD patterns of various monomer/OMLS and corresponding polymer nanocomposites.....	19
Figure 1.16.	TEM images of nanocomposites	19
Figure 1.17.	Schematic illustration of the intercalation process between a polymer melt and OMLS.....	21
Figure 1.18.	Representative WAXD of PS35/OMLS hybrid heated to 165 °C for various times.....	22

Figure 1.19.	Schematic representation of the dispersion process of OMLS in the PP matrix with the aid of PP-MA	24
Figure 1.20.	Surfactants used: N-N dialkyl dimethyl ammonium chloride (left), Alkyl dimethyl benzyl ammonium chloride (right).....	25
Figure 1.21.	Chemical Structure of Azo-initiator 2,2'-Azobis(2-methyl propionamide)..	26
Figure 1.22.	Temperature dependence of G', G'', and tan d for PP-MA matrix and various PPCNs.....	28
Figure 1.23.	Tensile characterization of the PP/fMMT nanocomposites.....	29
Figure 1.24.	TGA curves for polystyrene, PS and the nano composites.....	30
Figure 1.25.	Formation of tortuous path in PLS nanocomposites.....	32
Figure 1.26.	UV-vis transmittance spectra of PVA/MMT nanocomposites containing 4 and 10 wt.% MMT	37
Figure 2.1.	Clay treatment procedure	37
Figure 3.1.	¹ H-NMR spectra of water soluble azo-initiator before (left) and after (right) quaternization with dimethylsulfide.....	42
Figure 3.2.	DSC thermogram of water soluble azo-initiator before (left) and after (right) quaternization with dimethylsulfide.....	45
Figure 3.3.	Comparison of WAXD patterns of treated clays and commercial grades	43
Figure 3.4.	Thermogravimetric Analysis of Na ⁺ -MMT treated with two surfactants...	45
Figure 3.5.	WAXD patterns of surfactant-initiator pairs.....	46
Figure 3.6.	Thermogravimetric Analysis of surfactant-initiator pairs.....	47
Figure 3.7.	SEM image of MC1-polystyrene masterbatch.....	48
Figure 3.8.	WAXD patterns of various melt blends.....	48
Figure 3.9.	Thermogravimetric analysis of melt blends.....	49

Fig.3.10 SEM image of unfilled SEBS (left) and MC1-MB nanocomposite.....	51
Fig. 3.11 SEM images of MC1-MB nanocomposite at higher magnification.....	52

LIST of TABLES

Table 1.1.	Chemical Formula and Characteristics of commonly used Clays.....	7
Table 1.2.	Summary of melt intercalation of M2C18 and F2C18 with styrene derivative polymers.....	23
Table 1.3.	HDT of PP/MMT nanocomposites and the respective unfilled PP.....	30
Table 1.4.	Cone calorimeter data of various polymers and their nanocomposites with OMLS.....	31
Table 2.1.	Table of clay modifier contents.....	37
Table 3.1.	Mechanical properties of nanocomposites.....	50

ABBREVIATIONS

1,1- bis, t-butyl peroxy

2,2'-AZOBIS, 2-methyl propionamide

2C18, dioctadecyldimethylammonium

BTC 1218-50, Alkyl dimethyl benzyl ammonium chloride

C18, octadecylammonium

CEC, cation exchange capacity

CL, ϵ -caprolactone

DSC, differential scanning calorimetry

DMA, dynamic mechanical analysis

DMF, dimethylformamide

EPDM, ethylene propylene diene methylene linkage rubber

EB, ethylene and butylene

F, fluorohectorite

FR, flame retardants

G', storage modulus

G'', loss modulus

G''/G', $\tan \delta$; the ratio (dikkat)

HDPE, high-density polyethylene

HMW, high molecular weight

HDT, heat distortion temperature

HRR, heat release rate

MA, maleic anhydride

MB, masterbatch

MC2, BTC 1218-50-untreated V-50

MC4, BTC 1218-50-treated V-50

MC1, tequart DSM-treated V-50

MC6, tequart DSM-untreated V-50

MC, modified clay

MMA, methyl methacrylate

MPA, mega pascal

MMT, montmorillonite

N6, nylon-6

NA+-MMT, na-montmorillonite

NMR, nuclear magnetic resonance

OC, organoclays

OMLS, organically modified layered silicate

PCN, polymer-clay nanocomposites

PEO, polyethylene oxide

PVA, poly(vinyl alcohol)

PLS, polymer/layered silicate

PVP, poly(N-vinyl pyrrolidone)

PCL, poly(ϵ -caprolactone)

PLA, polylactide

PDMS, poly(dimethylsiloxane)

PS, polystyrene

PMMA, poly(methyl methacrylate)

PP, polypropylene

PP-MA, maleic anhydride grafted polypropylene;

PPCN, pp/clay nanocomposites

QA+, quaternary ammonium cation

QC18, octadecyltrimethylammonium

SEBS, styrene-block-ethylenebutylene-block-styrene

SBR, 1,3 styrene-butadiene copolymer

SBS, poly(styrene-block-butadiene-block-styrene)

SIS, poly(styrene-block-isoprene-block-styrene)

STN, methyltrioctylammonium modified smectite

SPN, diethylmethylammonium modified smectite

S, styrene

SAP, saponite

SEBS-MA, maleic anhydride grafted sebs

TPE, thermoplastic elastomers

TEQUART DSM, n-n dialkyl dimethyl ammonium chloride

TEM, transmission electron microscopy

TGA, thermogravimetric analysis

THF, tetrahydrofuran

WAXD, wide angle X-ray diffraction

CHAPTER 1

INTRODUCTION

1.1. SEBS Overview

SEBS (Styrene-block-ethylenebutylene-block-Styrene) is a member of material class called Thermoplastic elastomers (TPE). TPE is an elastomeric material with the processing characteristics of a thermoplastic and the performance properties of a thermoset rubber.[1] In other words, TPEs are fabricated by techniques such as extrusion, injection molding, and etc. used for thermoplastics like polypropylene and polyethylene but they exhibit the properties of a conventional rubber such as natural rubber (1,4 Polyisoprene), SBR (1,3 Styrene-butadiene copolymer) or EPDM (Ethylene-propylene-dien terpolymer). They are easily recycled, reshaped, and processed. They have shorter molding cycles and more fabricated parts per unit weight of material when compared with thermoset rubbers. So they are the replacements of vulcanized rubber or some other thermosets that could be partially or could not be recycled at all. According to World Thermoplastic Elastomers Global Market report presented by Global Information, Inc World demand for TPEs is forecasted to expand 7.5 percent per year to 2.6 million metric tons in 2006, valued at US\$12 billion.[2]

The idea behind thermoplastic elastomers is the notion of a reversible crosslink. Crosslinks in thermoset rubber are covalent which means that they chemically bond the

polymer chains together into one molecule. The reversible crosslinks in TPEs uses noncovalent, or secondary interactions between the polymer chains to bind them together. These interactions include hydrogen bonding and ionic bonding. When the material is heated, the crosslinks are broken and this allows the material to be processed, and most importantly, recycled. When it cools again, the crosslinks reform.[3]

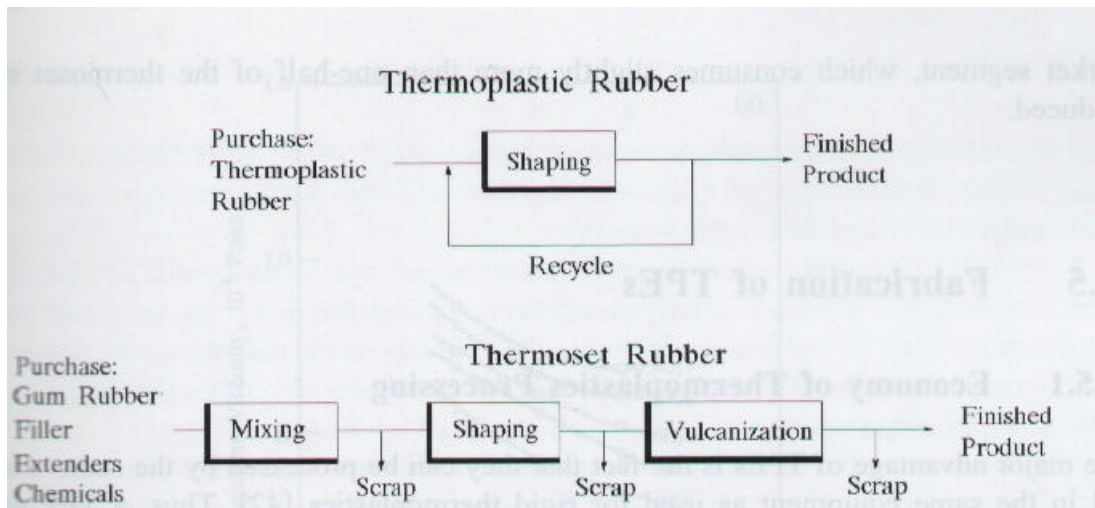


Fig.

1.1 Comparison of TPE fabrication to that of thermoset rubber.[1]

However, because this transition to final form is reversible, some end-use properties of SEBS such as compression set, and upper service temperature are not so good as those of the corresponding thermoset rubbers. Because of this, applications of styrenic thermoplastic elastomers are in areas where these properties are less important (footwear, wire insulation, candles, adhesives, polymer blending, soft touch goods) but they have not penetrated other markets such as automobile tires.

Since the introduction of alkyl lithium initiators' usage for isoprene polymerization and research about varying molecular weighed triblock copolymers of polystyrene and isoprene by Shell development company, commercially production of SEBS became viable and SEBS has been a good candidate for replacement of traditional rubber goods.[4] Inorganic fillers like Calcite, talk and etc. have been incorporated in SEBS formulations in order to tailor some properties such as density and cost. But these fillers are in micron

range in size and as their percentage increases in formulations some of the properties such as elasticity decreases.

Development of a commercially viable method for SEBS-clay nanocomposites preparation; in other words, dispersing inorganic filler to polymer matrix in nano size, will improve properties such as flame retardancy, gas barrier properties, tensile strength, heat distortion temperature and etc.[5] Enhancement of the properties of SEBS will also rise possibility of increasing number of applications where SEBS fails against thermoset rubbers like high temperature resistant elastic automobile parts, window seals where compression set is critical or a football inner balloon which requires impermeability of gas molecules.

This study aims to successfully synthesize SEBS-clay nanocomposites with enhanced properties but with easy-to-find, cheap ingredients and easiest, most efficient and most commercially viable method. So a research route to find most efficient application has been followed. Starting point of such a challenge was to first accumulate previous work done on nanocomposite preparation and information about the properties of SEBS.

1.1.1 Structure

The structure of SEBS gives its Thermoplastic properties. There are multiphase compositions in which the phases are chemically bonded by block copolymerization. One of the phases is Polystyrene that is hard at room temperature but becomes fluid when the polymer is heated, whereas the other phase is a softer material that behaves like rubber at room temperature.[3] Two ends of the copolymer consists of Polystyrene segments and mid block is elastomeric b-ethylene-b-butylene copolymer.

Most of the polymers are thermodynamically incompatible even though they are part of a block copolymer. That is why phase separation occurs in SEBS. A typical demonstration of SEBS structure is in Fig. 1.2 here polystyrene end segments have formed separate spherical domains dispersed in a continuous elastomeric phase. Most of the polymer molecules have their end polystyrene segments in different domains. At room temperature, these polystyrene domains are hard and so act as physical crosslinks those tie

the elastomer chains together in a three-dimensional network. This resembles the network formed by vulcanizing conventional rubbers using chemical crosslinking agents. In the latter case, crosslinking is irreversible process; but in SEBS domains lose their strength when the material is heated or dissolved in solvents, allowing the polymer or its solution to flow. When the material is cooled or the solvent is evaporated, the domains become hard again, and the network regains its original integrity. In other words, in SEBS the formation of rubbery network is a reversible process.

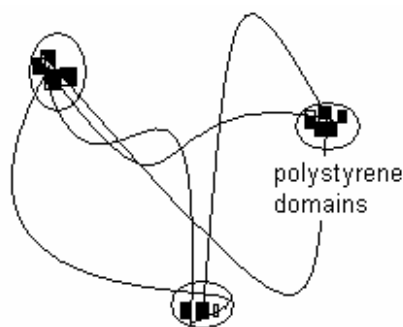


Fig. 1.2 Demonstration of SEBS structure.

1.1.2 Synthesis and Commercial Production

SEBS is made by anionic polymerization using an alkyl-lithium initiator (R-Li).[6] This first reacts with styrene monomer (Fig. 1.3):

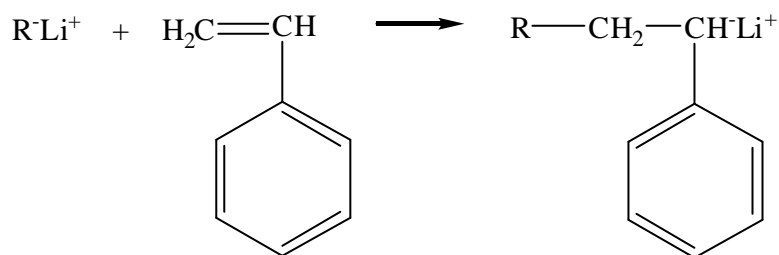


Fig. 1.3 Synthesis of SEBS step 1

The product now acts as an initiator for further polymerization (Fig. 1.4):

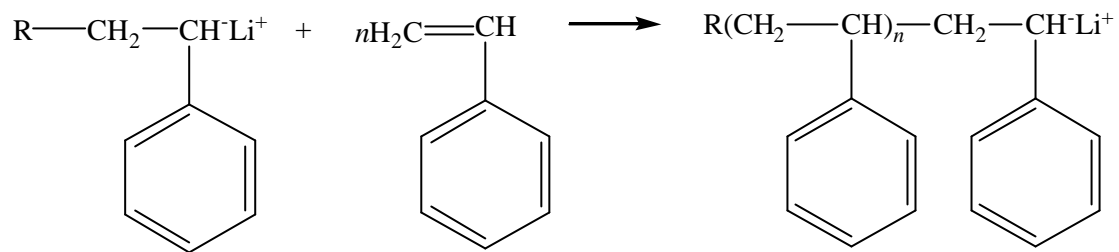


Fig. 1.4 Synthesis of SEBS step 2

This product (donated S^-Li^+) has been termed a living polymer because it can initiate further polymerization. If a second monomer, such as butadiene, is added, the following reaction occurs (Fig. 1.5):

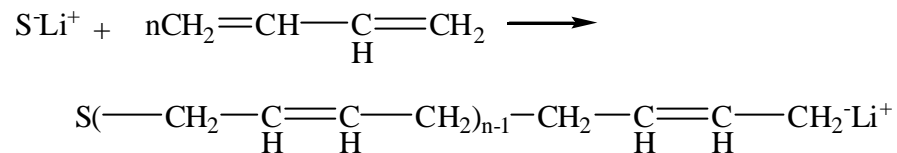


Fig. 1.5 Synthesis of SEBS step 3

This reaction product (donated $\text{S}^-\text{B}^-\text{Li}^+$) can then initiate a further reaction with added styrene monomer to give $\text{S-B-S}^-\text{Li}^+$, which in turn can be reacted with an alcohol R-OH , to give S-B-SH and LiOR .

The polymerization proceeds only in the absence of terminating agents such as oxygen, carbon dioxide, or water; therefore, polymerization is usually carried out in an inert hydrocarbon solvent and under a nitrogen blanket. These conditions produce polymers with narrow molecular weight distributions and precise molecular weights.[7]

There are only three common monomers namely; styrene, butadiene, isoprene that are easy to polymerize using this process. So only two poly(styrene-b-elastomer-b-styrene) block copolymers are directly produced on a commercial scale. These are poly(styrene-b-butadiene-b-styrene) SBS and poly(styrene-b-isoprene-b-styrene) SIS. In both cases the elastomer segments contain one double bond per molecule of original monomer.

These bonds are quite reactive and limit stability of product. In order to improve stability, micro structure modifiers are added, and as a result the polybutadiene midsegment is produced as a random mixture of two structural forms, the 1,4 and 1,2 isomers.[7] On

hydrogenation these isomers give a polymer that is essentially a copolymer of ethylene and butylene (EB):

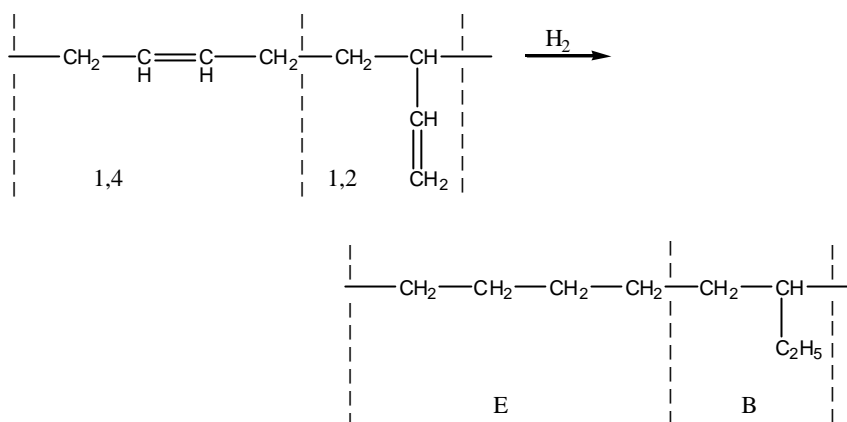


Fig. 1.6 Hydrogenation of the isomers.

SEBS is produced in this way and has excellent resistance to degradation.

1.2 Polymer-Clay Nanocomposites

Polymer-Clay (Layered Silicate) nanocomposites (PCN) are being greatly interested, both in industry and in academic world, because they usually improve remarkably the properties of materials when compared with virgin polymer or conventional micro and macro-composites. These improvements can include high modulus [5], increased strength and heat resistance [8], decreased gas permeability [9] and flammability [10], and increased biodegradability of biodegradable polymers [11]. Most of these properties are critical for SEBS and will broaden application areas or will add values to existing formulations.

Although the intercalation chemistry of polymers when mixed with appropriately modified layered silicate and synthetic layered silicates has long been known [12], the field of PCN has started to accelerate recently. Two major findings have increased the interest in these materials: first, the report from the Toyota research group of a Nylon-6 /montmorillonite (MMT) nanocomposite [13], for which very small amounts of layered silicate loadings resulted in improvements of thermal and mechanical properties; and second, the observation by Vaia et al. [14] that it is possible to melt-mix polymers with

layered silicates, without the use of organic solvents. Today, efforts are being conducted globally, using almost all types of polymer matrices.

1.2.1. Structure and properties of layered silicates

The commonly used layered silicates for the preparation of PCN belong to the same general family of 2:1 layered silicates. Their crystal structure consists of layers made up of two tetrahedrally coordinated silicon atoms located to an edge-shared octahedral sheet of either aluminum or magnesium hydroxide. The layer thickness is around 1 nm, and the lateral dimensions of these layers may vary from 30 nm to several microns or larger, depending on the particular layered silicate. Stacking of the layers leads to a regular van der Waals gap between the layers called the interlayer or gallery.

Isomorphic substitution within the layers (for example, Al^{3+} replaced by Mg^{2+} or Fe^{2+} , or Mg^{2+} replaced by Na^{1+}) generates negative charges that are counterbalanced by alkali and alkaline earth cations situated inside the galleries. This type of layered silicate is characterized by a moderate surface charge known as the cation exchange capacity (CEC), and generally expressed as mequiv/100 gm. This charge is not locally constant, but varies from layer to layer, and must be considered as an average value over the whole crystal.[15]

MMT, hectorite, and saponite are the most commonly used layered silicates. Layered silicates have two types of structure: tetrahedral-substituted and octahedral substituted. In the case of tetrahedrally substituted layered silicates the negative charge is located on the surface of silicate layers, and hence, the polymer matrices can react, interact more readily with these than with octahedrally substituted material.

Details about the structure and chemistry for these layered silicates are provided in Fig. 1.7 and Table 1.1. respectively. Two particular characteristics of layered silicates that are generally considered for polymer clay nanocomposites. The first is the ability of the silicate particles to disperse into individual layers. The second characteristic is the ability to fine-tune their surface chemistry through ion exchange reactions with organic and inorganic cations. These two characteristics are, of course, interrelated since the degree of dispersion of layered silicate in a particular polymer matrix depends on the interlayer cation.

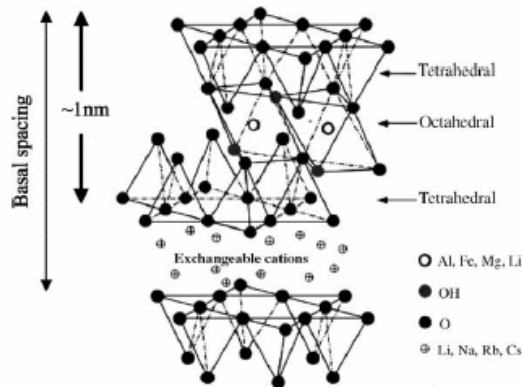


Fig. 1.7 Structure of 2:1 Phyllosilicates [20]

Table 1.1 Chemical Formula and Characteristics of commonly used Clays. [15]

2:1 phyllosilicates	Chemical formula	CEC (mequiv/100 g)	Particle length (nm)
Montmorillonite	$M_x(\text{Al}_{4-x}\text{Mg}_x)\text{Si}_8\text{O}_{20}(\text{OH})_4$	110	100–150
Hectorite	$M_x(\text{Mg}_{6-x}\text{Li}_x)\text{Si}_8\text{O}_{20}(\text{OH})_4$	120	200–300
Saponite	$M_x\text{Mg}_6(\text{Si}_8-x\text{Al}_x)\text{Si}_8\text{O}_{20}(\text{OH})_4$	86.6	50–60

M, monovalent cation; x, degree of isomorphous substitution (between 0.5 and 1.3).

1.2.2 Structure and properties of organically modified layered silicate (OMLS)

The physical mixture of a polymer and layered silicate may not form a nanocomposite. This situation is analogous to polymer blends, and in most cases separation into discrete phases takes place. In immiscible systems, which typically correspond to the more conventionally filled polymers, the poor physical interaction between the organic and the inorganic components leads to poor mechanical and thermal properties. In contrast, strong interactions between the polymer and the layered silicate in PLS nanocomposites lead to the organic and inorganic phases being dispersed at the nanometer level. As a result, nanocomposites exhibit unique properties not shared by their micro counterparts or conventionally filled polymers [5].

Pristine layered silicates usually contain hydrated Na^{1+} or K^{1+} ions [15]. Obviously, in this pristine state, layered silicates are only miscible with hydrophilic polymers, such as poly(ethylene oxide) (PEO) [16], or poly(vinyl alcohol) (PVA) [17]. To render layered

silicates miscible with other polymer matrices, one must convert the normally hydrophilic silicate surface to an organophilic one, making the intercalation of many engineering polymers possible. Generally, this can be done by ion-exchange reactions with cationic surfactants including primary, secondary, tertiary, and quaternary alkylammonium or alkylphosphonium cations. Alkylammonium or alkylphosphonium cations in the organosilicates lower the surface energy of the inorganic host and improve the wetting characteristics of the polymer matrix, and result in a larger interlayer spacing. Additionally, the alkylammonium or alkylphosphonium cations can provide functional groups that can react with the polymer matrix, or in some cases initiate the polymerization of monomers to improve the strength of the interface between the inorganic and the polymer matrix [18].

Traditional structural characterization to determine the orientation and arrangement of the alkyl chain was performed using wide angle X-ray diffraction (WAXD). Depending on the packing density, temperature and alkyl chain length, the chains were thought to lie either parallel to the silicate layers forming mono or bilayers, or radiate away from the silicate layers forming mono or bimolecular arrangements (Fig. 1.8) [19].

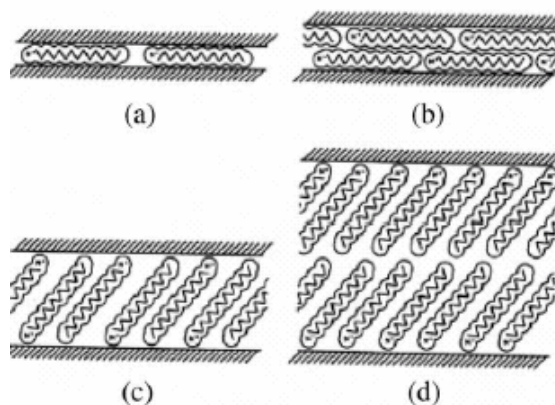


Fig. 1.8 Arrangements of Alkylammonium ions in mica-type layered silicates with different layer charges. Hatch areas silicate layers. [19]

1.2.3 Types of nanocomposites

In general, layered silicates have layer thickness on the order of 1 nm and a very high aspect ratio (e.g. 10–1000). A few weight percent of layered silicates that are properly dispersed throughout the polymer matrix thus create much higher surface area for polymer/filler interaction as compared to conventional composites. Depending on the strength of interfacial interactions between the polymer matrix and layered silicate (modified or not), three different types of polymer-layered silicate (PLS) nanocomposites are thermodynamically achievable (Fig. 1.9):

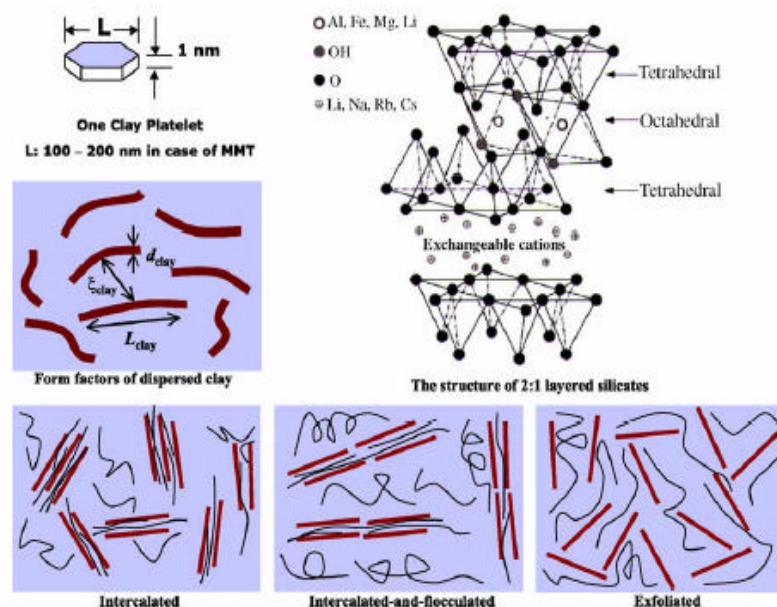


Fig. 1.9 Schematically illustration of three different types of thermodynamically stable PLS. [20]

Intercalated nanocomposites: in intercalated nanocomposites, the insertion of a polymer matrix into the layered silicate structure occurs in a crystallographically regular fashion, regardless of the clay to polymer ratio. Intercalated nanocomposites are normally interlayered by a few molecular layers of polymer. Properties of the composites typically resemble those of ceramic materials.

Flocculated nanocomposites: conceptually this is the same as intercalated nanocomposites. However, silicate layers are sometimes flocculated due to hydroxylated edge-edge interaction of the silicate layers.

Exfoliated nanocomposites: in an exfoliated nanocomposite, the individual clay layers are separated in a continuous polymer matrix by an average distances that depends on clay loading. Usually, the clay content of an exfoliated nanocomposite is much lower than that of an intercalated nanocomposite.

1.2.4 Techniques used for the characterization of Nanocomposites

Generally, the structure of nanocomposites has typically been established using WAXD analysis and transmission electron micrographic (TEM) observation. Due to its easiness and availability WAXD is most commonly used to probe the nanocomposite structure [5] and occasionally to study the kinetics of the polymer melt intercalation [21]. By monitoring the position, shape, and intensity of the basal reflections from the distributed silicate layers, the nanocomposite structure (intercalated or exfoliated) may be identified. For example, in an exfoliated nanocomposite, the extensive layer separation associated with the delamination of the original silicate layers in the polymer matrix results in the eventual disappearance of any coherent X-ray diffraction from the distributed silicate layers. On the other hand, for intercalated nanocomposites, the finite layer expansion associated with the polymer intercalation results in the appearance of a new basal reflection corresponding to the larger gallery height. In other words, the success of intercalation is mainly verified by the increase of the (001) interlayer distance (d-basal spacing) determined by WAXD.[22]

Although WAXD offers a convenient method to determine the interlayer spacing of the silicate layers in the original layered silicates and in the intercalated nanocomposites (within 1–4 nm), little can be said about the spatial distribution of the silicate layers or any structural non-homogeneities in nanocomposites. Additionally, some layered silicates initially do not exhibit well-defined basal reflections. Thus, peak broadening and intensity decreases are very difficult to study systematically. Therefore, conclusions concerning the mechanism of nanocomposites formation and their structure based solely on WAXD patterns are only tentative. On the other hand, TEM allows a qualitative understanding of the internal structure, spatial distribution of the various phases, and views of the defect structure through direct visualization. However, special care must be exercised to guarantee

a representative cross-section of the sample. The WAXD patterns and corresponding TEM images of three different types of nanocomposites are presented in Fig. 1.10.

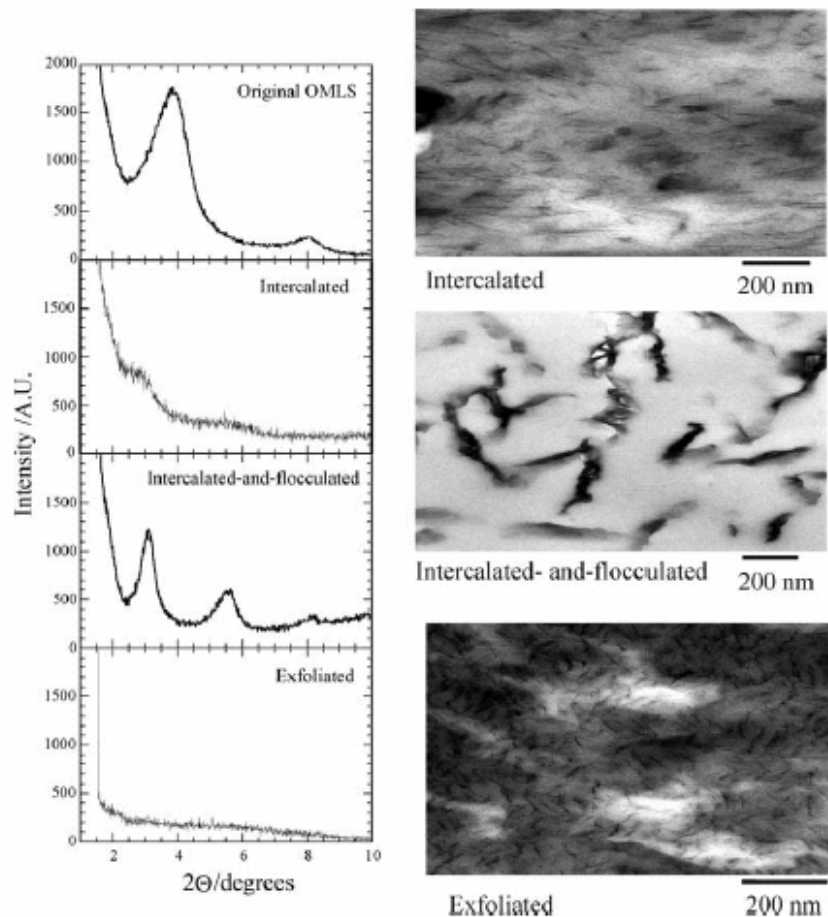


Fig. 1.10 WAXD patterns and TEM images of three different types of PCN. [8]

Both TEM and WAXD are essential tools for evaluating nanocomposite structure. However, TEM is time-intensive, and only gives qualitative information on the sample as a whole, while low-angle peaks in WAXD allow quantification of changes in layer spacing. Typically, when layer spacing exceed 6–7 nm in intercalated nanocomposites or when the layers become relatively disordered in exfoliated nanocomposites, associated WAXD features weaken to the point of not being useful.

Thermogravimetric analysis (TGA) is another essential tool for the characterization of PCN. TGA can be used first to investigate the intercalation efficiency in the treated clays since percentage of the surfactant embedded in the clay structure can be easily determined

by the idea that first surfactant will decompose as temperature increases. Second, TGA is used to quantify thermal stability of PCN. Onset of degradation is recorded commonly in order to identify the improvement in PCN when compared with original polymer.[23]

In this particular study, Differential Scanning Calorimetry (DSC) has been used. The reason that lies behind is the novel and alternate method that will be applied for PCN preparation. This method will be discussed in detail in the following sections but briefly DSC will be used to prove the existence of initiator molecules in clay galleries those will be used for polymerization reactions. DSC would also help us to investigate thermal behaviour of synthesized PCN.

1.2.5. Preparative methods and morphological study

Intercalation of polymers in layered hosts, such as layered silicates, has proven to be a successful approach to synthesize PCN. The preparative methods are divided into three main groups according to the starting materials and processing techniques. These are intercalation of polymer or pre-polymer from solution, in situ intercalative polymerization method, melt intercalation method.

1.2.5.1 Intercalation of polymer or pre-polymer from solution

This is based on a solvent system in which the polymer or pre-polymer is soluble and the silicate layers are swellable. The layered silicate is first swollen in a solvent, such as water, chloroform, or toluene. When the polymer and layered silicate solutions are mixed, the polymer chains intercalate and displace the solvent within the interlayer of the silicate. Upon solvent removal, the intercalated structure remains, resulting in PCN.

Water-soluble polymers, such as polyethylene oxide (PEO) [24], Polyvinyl alcohol (PVA) [25], poly(N-vinyl pyrrolidone) (PVP) [26] have been intercalated into the clay galleries using this method. Examples from non-aqueous solvents are nanocomposites of poly(ϵ -caprolactone) (PCL)/clay [27] and polylactide (PLA)/clay [28] in chloroform as a

co-solvent, and high-density polyethylene (HDPE) with xylene and benzonitrile [29]. Nematic liquid crystal PCNs have also been prepared using this method in various organic solvents, such as toluene and dimethylformamide [30]. The thermodynamics involved in this method are described in the following. For the overall process, in which polymer is exchanged with the previously intercalated solvent in the gallery, a negative variation in the Gibbs free energy is required. The driving force for the polymer intercalation into layered silicate from solution is the entropy gained by desorption of solvent molecules, which compensates for the decreased entropy of the confined, intercalated chains [31].

Using this method, intercalation only occurs for certain polymer/solvent pairs. This method is good for the intercalation of polymers with little or no polarity into layered structures, and facilitates production of thin films with polymer-oriented clay intercalated layers. However, from commercial point of view, this method involves the use of organic solvents, which is usually environmentally unfriendly and economically prohibitive. In 1992, Aranda and Ruiz-Hitzky [24] reported the first preparation of PEO/MMT nanocomposites by this method. They performed a series of experiments to intercalate PEO ($M_w=105$ g/mol) into Na^+ -MMT using different polar solvents: water, methanol, acetonitrile, and mixtures (1:1) of water/methanol and methanol/acetonitrile. In this method the nature of solvents is critical in facilitating the insertion of polymers between the silicate layers, polarity of the medium being a determining factor for intercalations [12]. The high polarity of water causes swelling of Na^+ -MMT, provoking cracking of the films. Methanol is not suitable as a solvent for high molecular weight (HMW) PEO, whereas water/ methanol mixtures appear to be useful for intercalations, although cracking of the resulting materials is frequently observed. PEO intercalated compounds derived from the homoionic $M+n$ -MMT and $M+n$ hectorite like Na^+ -MMT, can satisfactorily be obtained using anhydrous acetonitrile or a methanol/acetonitrile mixture as solvents.

The resulting PEO/silicate materials show good stability toward treatment with different solvents (e.g. acetonitrile, methanol, ethanol, water, etc.) in experiments carried out at room temperature for long time periods (24 h). In addition, the lack of PEO replacement by organic compounds having high affinity toward the parent silicate, such as dimethyl sulfoxide and crown ethers, indicates again the high stability of PEO-intercalated

compounds. On the other hand, treatment with salt solutions provokes the replacement of the interlayer cations without disturbing the PEO. For example, Na^+ ions in PEO/ Na^+ -MMT are easily replaced by NH_4^+ or $\text{CH}_3(\text{CH}_2)_2\text{NH}^{3+}$ ions, after treatment (2 h) at room temperature with an aqueous solution of their chloride, perchlorate and thiocyanate salts (1N solutions), in a reversible process. This would also increase the basal spacing of clay.

Wu et al. [32] reported the intercalation of PEO in Na^+ -MMT and Na^+ -hectorite using this method in acetonitrile, allowing the stoichiometric incorporation of one or two polymer chains in between the silicate layers and increasing the inter sheet spacing from 0.98 to 1.36 and 1.71 nm, respectively.

Poly(dimethylsiloxane)/MMT nanocomposites were synthesized by sonicating a mixture of silanolterminated poly(dimethylsiloxane) (PDMS) and a commercial organosilicate at room temperature for 2 min [33]. A schematic illustration of nanocomposite synthesis is shown in Fig. 1.11. Delamination of the silicate particles in the PDMS matrix was accomplished by suspending and sonicating the organosilicate in PDMS at room temperature. WAXD analyses of various nanocomposites revealed no distinct features at low scattering angles, indicating the formation of exfoliated nanocomposites.

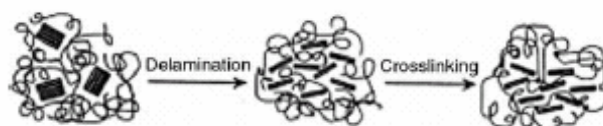


Fig. 1.11 Schematic illustration of nanocomposite synthesis. [34]

In another study, Usuki et al. used four different types of Organoclays (OC) in order to investigate the effect of OC on the structure and properties of polyimide/clay nanocomposites [34]. Hectorite, saponite, MMT, and synthetic mica were used as pristine layered silicates. The CEC of hectorite, saponite, MMT and synthetic mica are 55,100, 110, and 119 mequiv/100 gm, respectively, and all of them were modified with dodecylammonium cations using a cation exchange reaction. Parts a and b of Fig.- 1.12, respectively, represents the WAXD patterns of various OMLS and corresponding nanocomposites of polyimide in the range of $2\theta = 2-10^\circ$. WAXD patterns (Fig. 1.12-b)

revealed that the nanocomposites prepared with MMT or mica clay did not show any clear peaks corresponding to the exfoliated structure, while nanocomposites prepared with hectorite or saponite clay show small peaks, indicating that some portions of OC were stacked. The reason why MMT or mica dispersed homogeneously in the polyimide matrix was not explained properly by the authors, but there may be a greater interaction between the polyimide matrix and the organically modified MMT or synthetic mica compared to that of the polyimide matrix and organically modified hectorite or saponite clay.

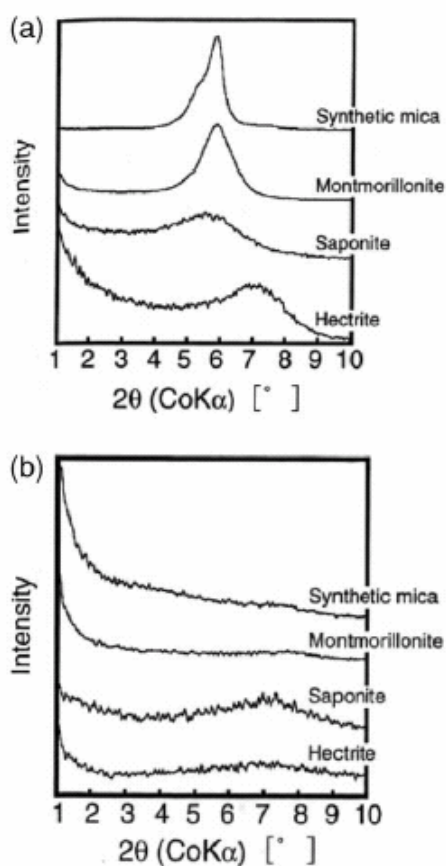


Fig. 1.12 WAXD patterns of (a) four different organo clays and (b) corresponding nanocomposites [34]

1.2.5.2 In situ intercalative polymerization method.

In this method, the layered silicate is swollen within the liquid monomer or a monomer solution so the polymer formation can occur between the intercalated sheets. Polymerization can be initiated either by heat or radiation, by the diffusion of a suitable initiator, or by an organic initiator or catalyst fixed through cation exchange inside the interlayer before the swelling step.

Although inter-lamellar polymerization techniques using appropriately modified layered silicate or synthetic layered silicates [12] have long been known, the field of PCN gained momentum since the report of a N6/MMT nanocomposite from the Toyota research group [13], where very small amounts of layered silicate loadings resulted improvements in thermal and mechanical properties. They first reported the ability of a γ -amino acids ($\text{COOH}-(\text{CH}_2)_{n-1}-\text{NH}_2^+$, with $n = 2; 3, 4, 5, 6, 8, 11, 12, 18$) modified Na^+ -MMT to be swollen by the ϵ -caprolactam monomer at 100°C and subsequently initiate its ring opening polymerization to obtain N6/MMT nanocomposites [35]. For the intercalation of ϵ -caprolactam, they chose the ammonium cation of γ -amino acids because these acids catalyze ring-opening polymerization of ϵ -caprolactam. The number of carbon atoms in a γ -amino acids has a strong effect on the swelling behavior as reported in Fig. 1.13, indicating that the extent of intercalation of ϵ -caprolactam monomer is high when the number of carbon atoms in the γ -amino acid is high. Fig. 1.14 represents the conceptual view of the swelling behavior of a γ -amino acid modified Na^+ -MMT by ϵ -caprolactam.

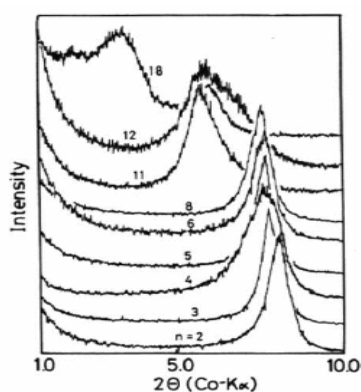


Fig. 1.13 WAXD patterns of γ amino acid ($\text{COOH}-(\text{CH}_2)_{n-1}-\text{NH}_2$) modified Na^+ -MMT.[35]

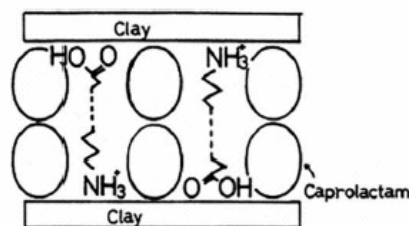


Fig. 1.14 Swelling behaviour of γ -amino acid modified MMT by ϵ -caprolactam [35]

For the preparation of PCL-based nanocomposites, Messersmith and Giannelis [36] modified MMT using protonated aminolauric acid and dispersed the modified MMT in liquid ϵ -caprolactam before polymerizing at high temperature. The nanocomposites were prepared by mixing up to 30 wt% of the modified MMT with dried and freshly distilled ϵ -caprolactam for a couple of hours, followed by ring opening polymerization under stirring at 170 °C for 48 h.

Chen et al. [38] used this PCL-based nanocomposites synthesis technique for the preparation of segmented polyurethane/clay nanocomposites based on diphenylmethane diisocyanate, butanediol and preformed polycaprolactone diol. They succeeded in producing a material in which the nano-filler acts as a multifunctional chain extender, inducing the formation of a star-shaped segmented polyurethane.

Pantoustier et al. [39] also used the in situ intercalative polymerization method for the preparation of PCL-based nanocomposites. They compared the properties of nanocomposites prepared using both pristine MMT, and γ -amino dodecanoic acid modified MMT. For nanocomposite synthesis, the desired amount of pristine MMT was first dried under vacuum at 70 °C for 3 h. A given amount of ϵ -caprolactam was then added to a polymerization tube under nitrogen and the reaction medium was stirred at room temperature for 1 h. A solution of initiator ($\text{Sn}(\text{Oct})_2$ or $\text{Bu}_2\text{Sn}(\text{OMe})_2$) in dry toluene was added to the mixture in order to reach a $[\text{monomer}]/[\text{Sn}]$ molar ratio equal to 300. The polymerization was then allowed to proceed for 24 h at room temperature. The inorganic content of the composite was measured by TGA. After polymerization, a reverse ion-exchange reaction was used to isolate the PCL chains from the inorganic fraction of the nanocomposite. A colloidal suspension was obtained by stirring 2 g of the nanocomposite in 30 ml of THF for 2 h at room temperature. A solution of 1 wt% of LiCl in THF was prepared separately. The nanocomposite suspension was added to 50 ml of the LiCl

solution and left to stir at room temperature for 48 h. The resulting solution was centrifuged at 3000 rpm for 30 min. The supernatant was then decanted and the remaining solid washed in 30 ml of THF followed by centrifugation. The combined supernatant was concentrated and precipitated from petroleum ether. The white powder was dried in vacuum at 50 °C. The polymerization of CL with pristine MMT gives PCL with a molar mass of 4800 g/mol and a narrow distribution. For comparison, the authors also conducted the same experiment without MMT, but found that there is no CL polymerization. These results demonstrate the ability of MMT to catalyze and to control CL polymerization, at least in terms of a molecular weight distribution that remains remarkably narrow.

Okamoto et al. [40,41] used organically modified smectite clays for the preparation of PMMA and polystyrene (PS) nanocomposites. Organically modified smectite clays (SPN and STN) were prepared by replacing Na⁺ smectite with Qa⁺ (quaternary ammonium salt), oligo (oxypropylene), diethylmethylammonium cation (SPN) or methyltrioctylammonium cation (STN) by exchange reaction. In a typical synthesis, both lipophilized smectite clays (SPN and STN) were dispersed in methyl methacrylate (MMA) and styrene (S) via ultrasonication at 25 °C for 7 h to obtain suspensions.

After that t-butyl peroxy-2-ethylhexanate and/or 1,1- bis (t-butyl peroxy) cyclohexane as an initiator was added to the suspensions and then free-radical polymerization was carried out in the dark at 80 °C for 5 h (for MMA) and at 100 °C for 16 h (for S) in a silicon oil bath. For comparison, the authors also prepared PMMA and/or PS including QA⁺ under the same conditions. WAXD analyses were performed directly from the suspensions of MMA/SPN, MMA/STN and S/SPN, and corresponding nanocomposites.

From WAXD patterns of the MMA/STN suspension (Fig. 1.15 a), higher-order peaks corresponding to $d_{(002)}$ and $d_{(003)}$ are clearly observed along with a $d_{(001)}$ peak, suggesting MMA intercalated into the STN gallery without the loss of layer structure, while the corresponding nanocomposite, PMMA/STN, exhibits a rather broad Bragg peaks, indicating the formation of a disordered intercalated structure.

In contrast, for the MMA/SPN suspension (Fig. 1.15b), the absence of any Bragg diffraction peaks indicates that the clay has been completely exfoliated or delaminated in the suspension. A similar pattern was observed in the case of the corresponding PMMA/SPN nanocomposite but with a small remnant shoulder as shown in Fig. 1.15b. At

the other extreme, the S/SPN suspension shows a small remnant shoulder that leads to the formation of a disordered intercalated structure, while the corresponding polymer nanocomposite shows strong WAXD diffraction implying the formation PS/SPN of an intercalated structure (Fig. 1.15c). But for all systems, the 2 θ peaks for nanocomposites are shifted to higher angle.

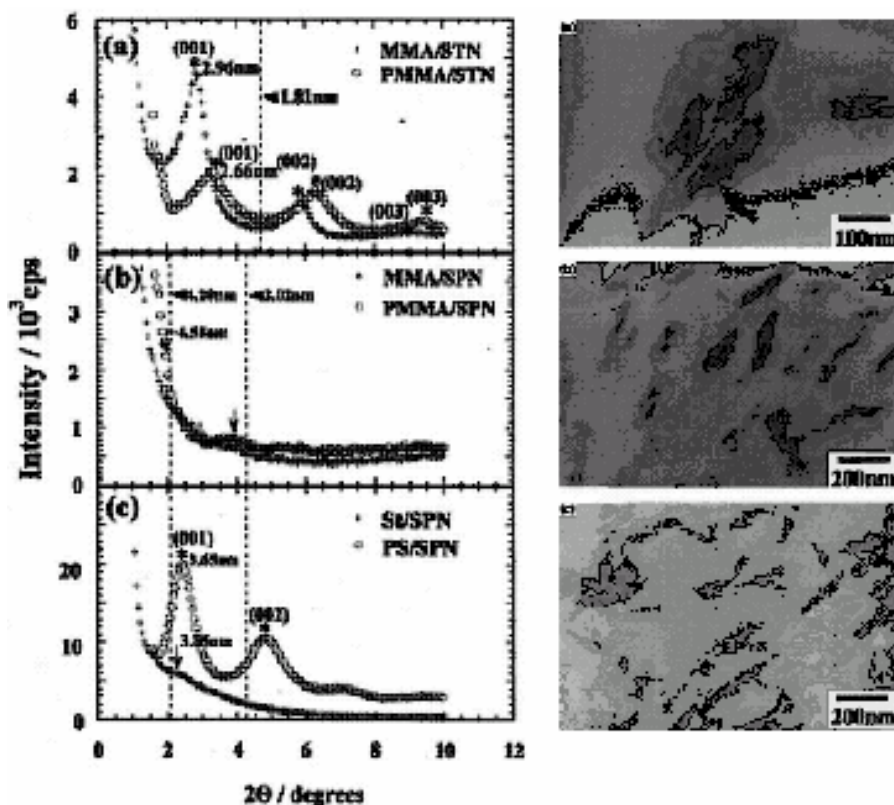


Fig. 1.15 (left) WAXD patterns of various monomer/OMLS and corresponding polymer nanocomposites. The dashed lines indicate location of silicate reflections of OMLS from suspensions and nanocomposites. The asterisk indicates the position of reflections from suspensions and nanocomposites. The arrows indicate a small or weak peak. [40]

Fig. 1.16 (right) TEM images of nanocomposites: (a) PMMA/STN, (b) PMMA/SPN, (c) PS/SPN. The arrow in panel (a) indicates the oriented collection of STN silicate layers. [40]

This behavior may be due to the volume shrinkage of monomers (5% in case of MMA and 3% in case of S) after polymerization. Fig. 1.16 represents the TEM bright field images of various nanocomposites, corresponding to the WAXD patterns as presented in Fig. 1.15. In the case of the PMMA/STN nanocomposite, individual silicate layers are stacked together and nicely dispersed in the PMMA matrix. Some areas (as indicated by the

arrow in Fig. 1.16a appear to contain an oriented collection of 10–20 parallel layers with a basal spacing of about 3 nm, which was consistent with the WAXD data. The PMMA/SPN nanocomposite (Fig. 1.16b) shows stacked silicate layers of about 200 nm length and about 40–50 nm thickness that consist of about 10 parallel individual silicate layers, and are randomly distributed in the matrix.

On the other hand, in the case of the PS/SPN nanocomposite system (Fig. 1.16c), a stacking of two to three silicate layers, with a distance of 4 nm are dispersed in the PS-matrix. Because of the difference between PS and PMMA matrices towards the compatibility with SPN, the final structure of the nanocomposites is different. As revealed by WAXD pattern, the PS chains are intercalated in the narrow space of the oriented collections of parallel silicate layers.

1.2.5.3 Melt Intercalation

This method involves annealing, statically or under shear, a mixture of the polymer and organically modified layered silicate (OMLS) above the softening point of the polymer. This method has great advantages over either in situ intercalative polymerization or polymer solution intercalation. First, this method is environmentally favored due to the absence of organic solvents. Second, it is compatible with current industrial process, such as extrusion and injection molding. The melt intercalation method allows the use of polymers which were previously not suitable for in situ polymerization or solution intercalation.

Recently, the melt intercalation technique has become the standard for the preparation of PCN. During polymer intercalation from solution, a relatively large number of solvent molecules have to be desorbed from the host to accommodate the incoming polymer chains. Therefore, there are many advantages to direct melt intercalation over solution intercalation. For example, direct melt intercalation is highly specific for the polymer, leading to new hybrids that were previously inaccessible. In addition, the absence of a solvent makes direct melt intercalation an environmentally sound and an economically favorable method for industries from a waste perspective. Fig. 1.17 represents a schematic

illustration of nanocomposite formation by direct melt intercalation in OMLS. This process involves annealing a mixture of the polymer and OMLS above the softening point of the polymer, statically or under shear. While annealing, the polymer chains diffuse from the bulk polymer melt into the galleries between the silicate layers. A range of nanocomposites with structures from intercalated to exfoliate can be obtained, depending on the degree of penetration of the polymer chains into the silicate galleries. So far, experimental results indicate that the outcome of polymer intercalation depends critically on silicate functionalization and constituent interactions. The critical issues are that (a) an optimal interlayer structure on the OMLS, with respect to the number per unit area and size of surfactant chains, is most favorable for nanocomposite formation, and (b) polymer intercalation depends on the existence of polar interactions between the OMLS and the polymer matrix.

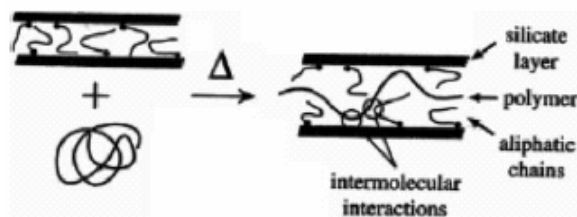


Fig. 1.17 Schematic illustration of the intercalation process between a polymer melt and OMLS. [31]

PS was the first polymer used for the preparation of nanocomposites using the melt intercalation technique with alkylammonium cation modified MMT [14]. In a typical preparative method, PS was first mixed with the host OMLS powder, and the mixture was pressed into a pellet, and then heated under vacuum at 165 °C. This temperature is well above the bulk glass transition temperature of PS, ensuring the presence of a polymer melt. Fig. 1.18 represents the WAXD patterns of the PS35 ($M_w=35000$)/OMLS hybrid before, and after 2, 5, 15 and 25 h of heating. The WAXD patterns of the hybrid before heating show peaks characteristic of the pure OMLS, and during heating the OMLS peaks were progressively reduced while a new set of peaks corresponding to the PS/OMLS appeared. After 25 h, the hybrid exhibits a WAXD pattern corresponding predominantly to that of the

intercalated structure. The same authors also carried out the same experiment under the same experimental conditions using Na⁺-MMT, but WAXD patterns did not show any intercalation of PS into the silicate galleries, emphasizing the importance of polymer/OMLS interactions. They also attempted to intercalate a solution of PS in toluene with the same OMLS used for melt intercalation, but this resulted in intercalation of the solvent instead of PS. Therefore, direct melt intercalation enhances the specificity for the intercalation of polymer by eliminating the competing host-solvent and polymer-solvent interactions. Further research by Vaia et al. [42] demonstrated the dispersion of various types of OMLS in a PS matrix. Li-fluorohectorite (F) (CEC = 150 mequiv/100 g), saponite (sap) (100 mequiv/100 g), and Na⁺-MMT (880 mequiv/100 g) were accordingly modified using various ammonium cations such as dioctadecyldimethylammonium (2C18), octadecyltrimethylammonium (qC18) octadecylammonium (C18), and a series of primary alkylammonium cations with carbon chains of 6, 9–16 and 18 carbon atoms. The nanocomposites were prepared using procedure as described above. After annealing, they found that FC18, F2C18, MMT2C18 and sap2C18 with PS yielded intercalated nanocomposite systems, however, with MMT C18, and sap C18, it resulted in immiscible, non-intercalated systems. Decreasing the host area per octadecyl chain, as with F2C18, also led to a non-intercalated system. Thus, on the basis of these results, it is established that an intermediate range of interlayer chain conformations are the most favorable for PS melt intercalation.

In order to understand the intermolecular interaction, Vaia et al. [42] also performed melt intercalation of F2C18 and MMT2C18 with various styrene derivative polymers. Table 1.2 represents these results. All the polymers are immiscible with F2C18. All polymers except PVCH form intercalated nanocomposite with MMT2C18, indicating that the structure of the pendent group on the polymer chain greatly affects nanocomposite formation.

Recently, a series of experiments has been designed and conducted by Beyer et al. [43] to construct a model for the morphological behavior of PCN, where a PCN is composed of a PS homopolymer, MMT and PS used as surfactant modifiers. The effect of surfactant length on the morphology of PCN was examined using an especially synthesized PS modified MMT as a model surfactant.

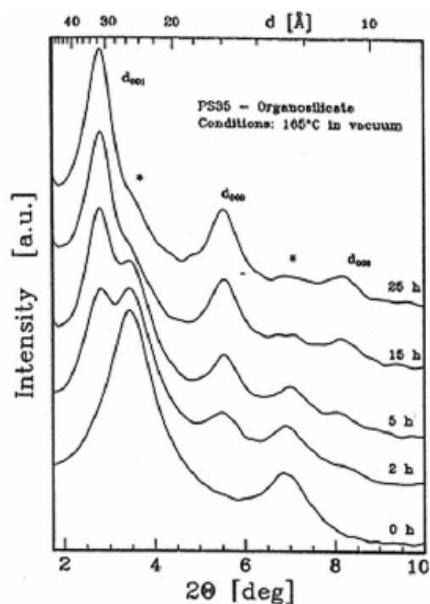
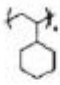
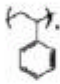
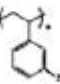
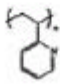


Fig. 1.18 Representative WAXD of PS35/OMLS hybrid heated to 165 °C for various times. Asterisks indicate the positions of the basal reflections from the pristine OMLS [14]

WAXD data showed the PS homopolymer did not intercalate into the PS modified MMT. This finding is consistent with the results for autophobic dewetting that occurs with densely grafted polymer brushes, based on high surfactant coverage within the layered silicate galleries.

Table 1.2 Summary of melt intercalation of M2C18 and F2C18 with styrenederivative polymers.

Polymer		Net gallery height increase (nm)	
		M2C18	F2C18
PVCH		0.00	0.00
PS		0.82	0.00
PS1Br		0.96 ^a	0.00
PVP		1.00 ^a	0.00

Today, propylene (PP) is one of the most widely used polyolefin polymers. Since it has no polar groups in the chain, direct intercalation of PP in the silicate galleries is impossible. Overcoming this difficulty, Usuki et al. [44] first reported a novel approach to prepare PP/clay nanocomposites (PPCNs) using a functional oligomer (PP-OH) with polar telechelic OH groups as a compatibilizer. In this approach, PP-OH was intercalated between the layers of 2C18 MMT, and then the PP-OH/2C18-MMT was melt mixed with PP to obtain the nanocomposite with intercalated structure. Further study by the same group [45] reported the preparation of PP/MMT nanocomposites obtained by melt blending of PP, a maleic anhydride grafted PP oligomer (PP-MA), and clays modified with stearyl ammonium using a twin-screw extruder. In their study, they used two different types of maleic anhydride modified PP oligomer with different amounts of maleic anhydride groups and two types of organically modified clays to understand the miscibility effect of the oligomers on the dispersibility of the OMLS in the PP matrix, and to study the effect of hybridization on their mechanical properties when compared with neat PP and PPCNs without oligomers.

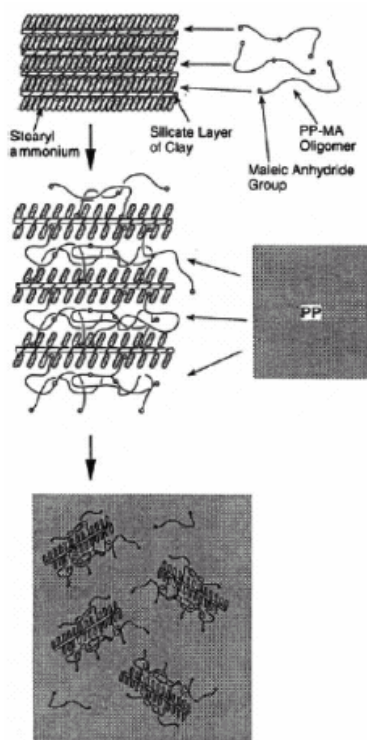


Fig. 1.19 Schematic representation of the dispersion process of OMLS in the PP matrix with the aid of PP-MA [45]

WAXD analyses and TEM observations established the intercalated structure for all nanocomposites. On the basis of WAXD patterns and TEM images, they proposed a possible mechanism for dispersion of intercalated clay layers in the PP matrix. Fig. 1.19 shows a schematic presentation of the mixing process of the three components i.e. PP, PP-MA, and OMLS into the nanocomposites. The present authors believe that the driving force of the intercalation originates from the maleic anhydride group and the oxygen groups of the silicate through hydrogen bonding.

Hasegawa et al. [46] found that maleic anhydride grafted PP (PP-MA) was able to intercalate into the inter-galleries of OMLS, similar to the functional oligomer, and described an approach for the preparation of PPCN by melt intercalation using a PPMA and organically modified clay. In a typical preparative method, PPCN pellets were prepared by melt blending pellets of PP-MA and the powder of C18-MMT at 200 °C, using a twin-screw extruder. WAXD patterns and TEM images showed that the silicate layers were exfoliated and uniformly dispersed in the PP-MA matrix. WAXD analysis of PPCN showed no peak representing dispersed C18-MMT in the PP-MA matrix. According to the authors, this means that the driving force of the PP-MA originates from the strong hydrogen bonding between the MA groups and the polar clay surface.

In this thesis, we combined melt intercalation method and in-situ intercalative polymerization method for producing SEBS/Clay nanocomposite. In such a challenge, the most appropriate clay type, surfactant for clay treatment, method for nanocomposite preparation have been investigated. This study searches the route to economically feasible, industrially applicable, and environmentally friendly way of producing SEBS/Clay nanocomposites.

The starting point of the thesis was the selection of proper clay type for modification. Na⁺-MMT with the most suitable cation exchange capacity (CEC=110 meq/100g) and particle length (100-150 nm) pair among the clay types has been chosen. (Table 1.1). Saponite has a particle length of 50-60 nm which is smaller than that of MMT but a CEC smaller. On the other hand, Hectorite type allows allows more ions to exchange but bigger particles with a length of 200-300 nm.

Another issue was the surfactant selection for clay treatment. Two types of surfactants which are readily available and serve for detergent industry in softener

formulations have been used; N-N dialkyl dimethyl ammonium chloride and Alkyl dimethyl benzyl ammonium chloride. N-N dialkyl dimethyl ammonium chloride has a hydrogenated tail consisting of 16-18 Carbons. Alkyl dimethyl benzyl ammonium chloride has an alkyl length of 12-18 carbons. They have been used for their ability to exchange with Na^+ located in the interlayer spacing of MMT. Their efficiency in intercalating the clay galleries has been investigated via WAXD patterns. [12,18,40,41]

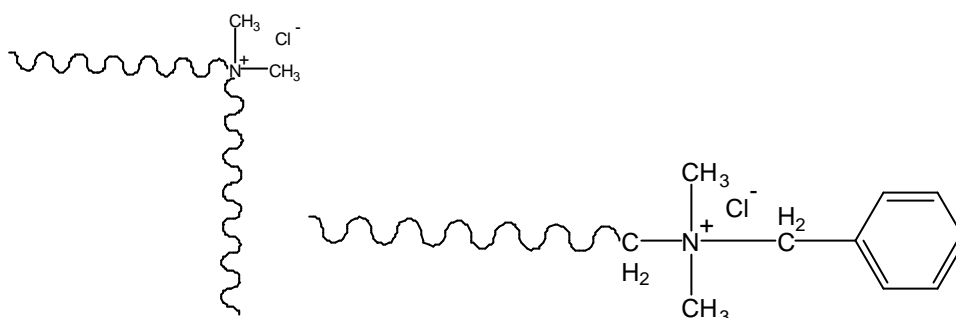


Fig. 1.20 Surfactants used: N-N dialkyl dimethyl ammonium chloride (left), Alkyl dimethyl benzyl ammonium chloride (up).

We have been inspired by the idea Toyota Research Group used for N6/Clay nanocomposites. They first reported the ability of a α -amino acids ($\text{COOH}-(\text{CH}_2)_{n-1}-\text{NH}_2^+$, with $n = 2; 3, 4, 5, 6, 8, 11, 12, 18$) modified Na^+ -MMT to be swollen by the ϵ -caprolactam monomer at 100°C and subsequently initiate its ring opening polymerization to obtain N6/MMT nanocomposites.[35] In this case, α -amino acid was a logical choice since it can guarantee the progress of polymerization within clay galleries so growing oligomer chains cause an increase in basal spacing of clay. But this case is unique for Nylon 6 and not applicable to all kind of monomers. As an alternative way, Pantoustier et al. [39] prepared a solution of initiator and added to reaction vessel at the desired time to begin polymerization. Here, another problem arises because of the location of polymerization initiation. Polymerization can take place anywhere in reaction media and possibility of oligomers intercalating the clay decreases. What is novel in our study was incorporation of a modified initiator that will both initiate the polymerization, and behave as a surfactant and locate within clay galleries like in the case of α -amino acids in PCL nanocomposites. We have methylated 2,2'-Azobis(2-methyl propionamide) (Fig. 1.21), a

water soluble initiator with Dimethylsulfate. Nitrogen atoms in both ends of the initiator molecule gain methyl groups and have a more ionic character . This water soluble methylated initiator would tend to exchange with Na^+ ions. Initiator was used with surfactant in equal compositions in order to realize this idea. Some excess amount was used to eliminate the efficiency loss caused by half life of initiator.

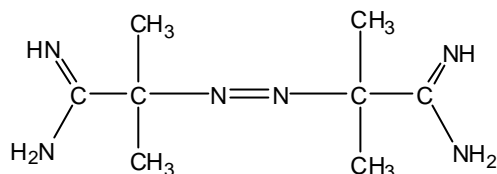


Fig. 1.21 Chemical Structure of Azo-initiator 2,2'-Azobis(2-methyl propionamide)

The second step was to polymerize a suitable monomer that will be compatible with SEBS. Na-MMT that was modified by the novel idea was added to styrene monomer and mixture was bulk polymerized. The product would be a nanocomposite masterbatch that will be compatible with the polystyrene domains (Fig.1.2) in SEBS. Then these masterbatches were melt mixed with SEBS in varying weight percentages. Classical attempt was also applied that MMT modified with only surfactant melt mixed with SEBS. Final method tested was incorporation of maleic anhydride grafted polymer in melt mixing process like Usuki et al. [45] had reported. They thought that OH groups in maleic anhydride could react with Oxygen atoms in MMT structure which would make intercalation of polymer chains into spacings easier. TEM images and WAXD patterns of experiments have been compared.

1.2.6 Nanocomposite Properties

Nanocomposites consisting of a polymer and layered silicate (modified or not) frequently exhibit remarkably improved mechanical and materials properties when compared to those of pristine polymers containing a small amount (≈ 5 wt%) of layered silicate. Improvements include a higher modulus[5], increased strength and heat

resistance[8], decreased gas permeability and flammability[9,10], and increased biodegradability of biodegradable polymers[11].

The main reason for these improved properties in nanocomposites is the stronger interfacial interaction between the matrix and layered silicate, compared with conventional filler-reinforced systems.

1.2.6.1. Mechanical properties

1.2.6.1.1 Dynamic mechanical analysis

Dynamic mechanical analysis (DMA) measures the response of a given material to an oscillatory deformation (here in tension–torsion mode) as a function of temperature. DMA results are composed of three parameters: (a) the storage modulus (G'); (b) the loss modulus (G''); and (c) $\tan \delta$; the ratio (G''/G'); useful for determining the occurrence of molecular mobility transitions, such as the glass transition temperature (T_g) [20].

Nam et al. [47] revealed the temperature dependence of G' ; G'' ; and $\tan \delta$ for the various PPCNs and corresponding PP-MA matrix. For all PPCNs, there is a strong enhancement of the moduli over the investigated temperature range, which indicates the plastic and elastic responses of PP towards deformation are strongly influenced in the presence of OMLS. Below T_g ; the enhancement of G' is clear in the intercalated PPCNs. The $\tan \delta$ curves for PPCNs show two peaks: one at 25 °C and another broad peak between 50 and 90 °C belonging to two relaxation states.

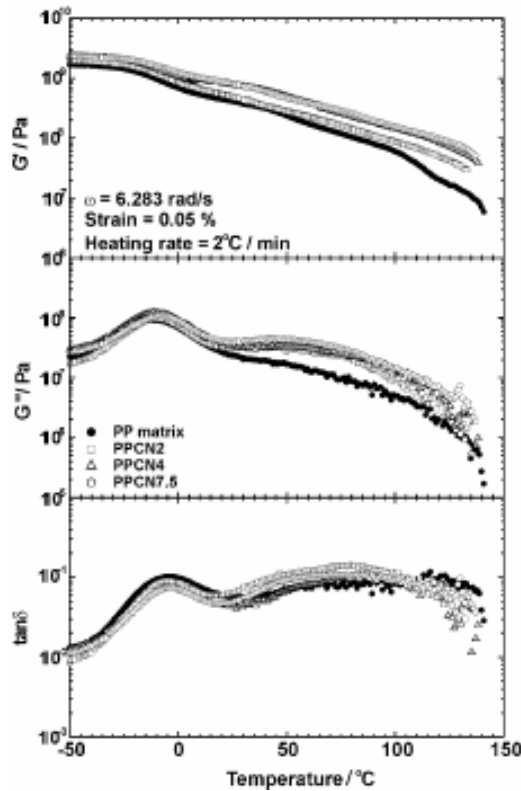


Fig. 1.22 Temperature dependence of G' , G'' , and $\tan \delta$ for PP-MA matrix and various PPCNs.

1.2.6.1.2 Tensile Properties

The tensile modulus of a polymeric material has been shown to be remarkably improved when nanocomposites are formed with layered silicates. Most of the studies report the tensile modulus as a function of clay content. Manias et al. [48] reported a study of a neat-PP/f-MMT composite compared to a PP/2C18-MMT ‘conventional macro’ composite. (Fig. 1.23) In PP/layered silicate nanocomposites, there is a sharp increase in tensile modulus for very small clay loading (≈ 3 wt%), followed by a much slower increase beyond a clay loading of 4 wt%. This is behavior characteristic of PCN. With an increase in clay content, strength does not change markedly compared to the neat-PP value, and there is only a small decrease in the maximum strain at break. Conventional composites of PP with the same fillers do not exhibit as much of an improvement in their tensile modulus.

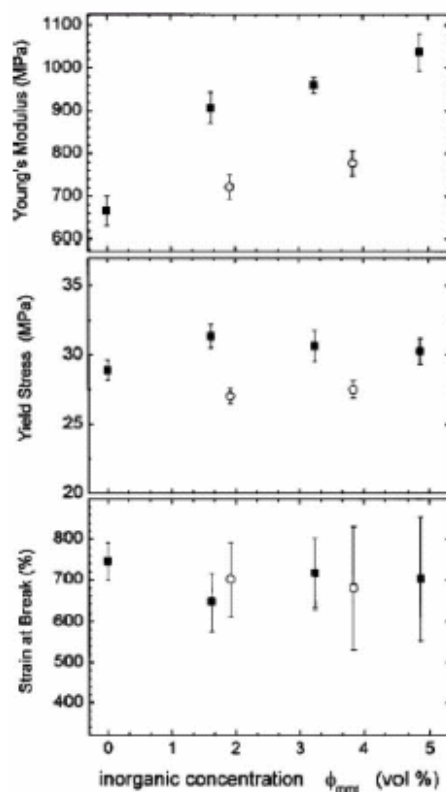


Fig.1.23 Tensile characterization of the PP/f-MMT nanocomposites. (filled squares) For Comparison, conventionally filled PP/2C18-MMT ‘macro’ composites are also shown. (unfilled circles) [48]

1.2.6.2 Heat distortion temperature

Heat distortion temperature (HDT) of a polymeric material is an index of heat resistance towards applied load. Most of the nanocomposite studies report HDT as a function of clay content. The previous study of Manias et al. also revealed that nano-dispersion of MMT in PP matrix promotes a higher HDT [48]. The HDT of PP and its nanocomposites based on f-MMT and alkylammonium modified MMT are summarized in Table 1.3. Like previous systems, there is a significant increase in HDT, from 109 °C for the neat PP to 152 °C for a 6 weight % of clay, after which the HDT of the nanocomposites levels off. This improvement in HDT for neat PP after nanocomposite preparation originates from the greater mechanical stability of the nanocomposite as compared to neat PP, since there is no increase in melting point of neat PP after nanocomposite preparation.

Table 1.3 HDT of PP/MMT nanocomposites and the respective unfilled PP. [48]

Organically modified mmt (wt%)	HDT (°C)	
	PP/f-MMT	PP/alkyl-MMT
0	109 ± 3	109 ± 3
3	144 ± 5	130 ± 7 ^a
6	152 ± 5	141 ± 7 ^b
9	153 ± 5	

1.2.6.3 Thermal Stability

The thermal stability of polymeric materials is usually studied by thermogravimetric analysis (TGA). The weight loss due to the formation of volatile products after degradation at high temperature is monitored as a function of temperature. When the heating occurs under an inert gas flow, a non-oxidative degradation occurs, while the use of air or oxygen allows oxidative degradation of the samples. Generally, the incorporation of clay into the polymer matrix was found to enhance thermal stability by acting as a superior insulator and mass transport barrier to the volatile products generated during decomposition.

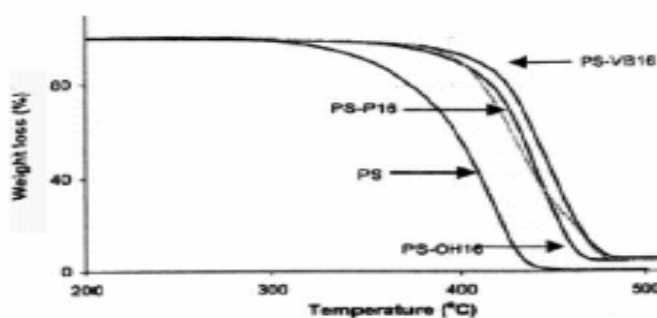


Fig. 1.24 TGA curves for polystyrene (PS), and the nanocomposites.[49]

Fig. 1.24 represents the TGA analysis of a phosphonium-PS nanocomposite compared with virgin PS. It shows that the thermal stability of the nanocomposite is enhanced relative to that of virgin PS [49], and the typical onset temperature of the degradation is about 50 °C higher for the nanocomposites.

1.2.6.4 Fire Retardant Properties

The Cone calorimeter is one of the most effective bench-scale methods for studying the fire retardant properties of polymeric materials. Fire-relevant properties such as the heat release rate (HRR), heat peak HRR, smoke production, and CO₂ yield, are vital to the evaluation of the fire safety of materials.

Table 1.4 represents the cone calorimeter data of three different kinds of polymer and their nanocomposites with MMT. As shown in Table 1.4, all of the MMT- based nanocomposites reported here exhibit reduced flammability. The peak HRR is reduced by 50–75% for N6, PS, and PP-g-MA nanocomposites [10]. According to the authors, the MMT must be nanodispersed for it to affect the flammability of the nanocomposites. However, the clay need not be completely delaminated. In general, nanocomposite flame retardant mechanism involves a high performance carbonaceous-silicate char, which builds up on the surface during burning. This insulates the underlying material and slows the mass loss rate of decomposition products.

Table 1.4 Cone calorimeter data of various polymers and their nanocomposites with OMLS.[10]

Sample (structure)	% residue yield (± 0.5)	Peak HRR (kW/m ²) ($\Delta\%$)	Mean HRR (kW/m ²) ($\Delta\%$)	Mean H_c (MJ/kg)	Mean SEA (m ² /kg)	Mean CO yield (kg/kg)
N6	1	1010	603	27	197	0.01
N6 nanocomposite 2% (delaminated)	3	686 (32)	390 (35)	27	271	0.01
N6 nanocomposite 5% (delaminated)	6	378 (63)	304 (50)	27	296	0.02
PS	0	1120	703	29	1460	0.09
PS-silicate mix 3% (immiscible)	3	1080	715	29	1840	0.09
PS-nanocomposite 3% (intercalated/delaminated)	4	567 (48)	444 (38)	27	1730	0.08
PSw/DBDPO/Sb ₂ O ₃) 30%	3	491 (56)	318 (54)	11	2580	0.14
PpgMA	5	1525	536	39	704	0.02
PpgMA-nanocomposite 2% (intercalated/delaminated)	6	450 (70)	322 (40)	44	1028	0.02
PpgMA-nanocomposite 4% (intercalated/delaminated)	12	381 (75)	275 (49)	44	968	0.02

Heat flux, 35 kW/m². H_c , specific heat of combustion; SEA, specific extinction area. Peak HRR, mass loss rate, and SEA data, measured at 35 kW/m², are reproducible to within $\pm 10\%$. The carbon monoxide and heat of combustion data are reproducible to within

1.2.6.5 Gas Barrier Properties

Clays are believed to increase the barrier properties by creating a maze or ‘tortuous path’ (Fig. 1.25) that retards the progress of the gas molecules through the matrix resin.[9] The direct benefit of the formation of such a path is clearly observed in polyimide/clay nanocomposites by dramatically improved barrier properties, with a simultaneous decrease in the thermal expansion coefficient [50]. The polyimide/layered silicate nanocomposites with a small fraction of OMLS exhibited reduction in the permeability of small gases, e.g. O₂, H₂O, He, CO₂, and ethylacetate vapors [50]. For example, at 2 wt% clay loading, the permeability coefficient of water vapor was decreased ten-fold with synthetic mica relative to pristine polyimide. By comparing nanocomposites made with layered silicates of various aspect ratios, the permeability was seen to decrease with increasing aspect ratio.

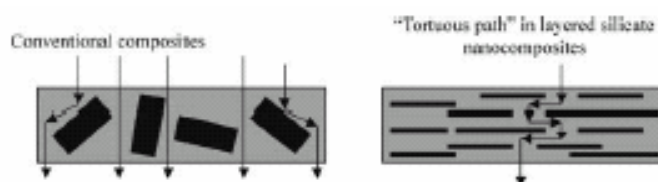


Fig. 1.25 Formation of tortuous path in PLS nanocomposites.[9]

1.2.6.6 Optical Transparency

Although layered silicates are microns in lateral size, they are just 1 nm thick. Thus, when single layers are dispersed (delaminated) in a polymer matrix, the resulting nanocomposite is optically clear in visible light. Fig.1.26 presents the UV/visible transmission spectra of pure PVA and PVA/Na⁺-MMT nanocomposites with 4 and 10 wt. % MMT. The spectra show that the visible region is not affected by the presence of the silicate layers, and retains the high transparency of PVA. For UV wavelengths, there is strong scattering and/or absorption, resulting in very low transmission of UV light. This behavior is not surprising, as the typical MMT lateral sizes are 50–1000 nm. Like PVA,

various other polymers also show optical transparency after nanocomposite preparation with OMLS [51,52].

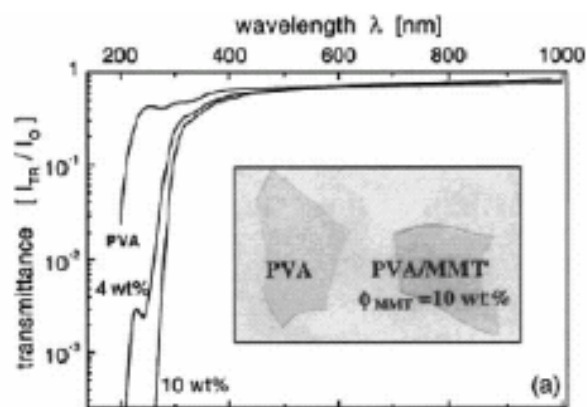


Fig. 1.26 UV-vis transmittance spectra of PVA/MMT nanocomposites containing 4 and 10 wt.% MMT [52]

CHAPTER 2

EXPERIMENT

This study searches the route to economically feasible, industrially applicable, and environmentally friendly way of producing SEBS/Clay nanocomposites.

Starting materials, synthesis procedure and technique, and characterization procedure are described in the following sections.

2.1. Materials

Most of the materials used in this study were supplied locally from Turkish companies in harmony with the objective. We believe that development of local Technologies for all kind of novel products independently is a key to make our country one of the leading research and development centers around the world.

2.1.1. Surfactants and clay

Surfactants used for clay treatment are easy-to find chemicals used in detergent formulations as a softener aid. Two kinds of surfactants were used; N-N dialkyl “di hydrogenated tallow” dimethyl ammonium chloride and Alkyl dimethyl benzyl ammonium chloride from two different companies. Two of them were supplied from Tekpar Kimyevi Maddeler San. Ve Tic. A.S. N-N dialkyl “di hydrogenated tallow” dimethyl ammonium chloride (**Tequart DSM**) was a wt. 75 % solution in water-isopropanol mixture.

Hydrogenated tallows were consisting of 65 % C18 and 35 % C16. Alkyl dimethyl benzyl ammonium chloride (**BTC 1218-50**) was wt. 50 % solution in water. Hydrogenated tallow was consisting of 56 % C12, 23 % C14, 11 % C16, 8% C18, and 2 % C10. In addition to them, two organically modified MMT were purchased for comparison purposes; Viscobent (Bensan A.S.) and Cloisite 15 A (Southern Clay Products, USA).

Na-Montmorillonite (Na^+ -MMT) was supplied from Bensan A.S. originated from Canakkale/Turkey. It has a Cation exchange capacity (CEC) of 120 meq/100g. Methanol used for cleaning and removal of unreacted species was technical grade from Sigma Aldrich Chemie GmbH, Germany.

2.1.2. SEBS, Styrene, Initiator, and others.

SEBS compound was supplied from Enplast A.S., one of the leading compounders of Turkey. It is a standard 60 shore A hardness, transparent grade with a density of 0.90 g/cm^3 , and a melt flow index of 3-5 g/10 min. under the trade name SN 3100 60A 000 T0. Maleic Anhydrite grafted SEBS (SEBS-MA) was Kraton G 1901X of Shell Company, U.S.A.

Styrene monomer was an industrial grade. Initiator was a water-soluble cationic azo-Initiator of Wako-Chemicals, Japan sold under the trade name V-50. V-50's chemical formula is 2,2'-Azobis(2-methyl propionamide)dihydrochloride with a molecular weight of 271.19 g/mol and a half-life of 10 hours at 56 °C water. Dimethylformamide (DMF), ethyl acetate and dimethylsulfide used for initiator modification was supplied from Merck Chemicals, Germany Sigma Aldrich Chemical Company, Germany and Gemsan A.S., Turkey respectively.

2.2. Experimental Procedure

2.2.1 Clay Treatment

Modification of Na-montmorillonite (Na^+ -MMT), was done by several different surfactant, and surfactant-modified initiator combination in order to make a comparison and to find the most efficient surfactant, or surfactant-modified initiator pair in terms of their capability to increase the interlayer spacing of between the end products. First step was quarternization of initiator V-50 so that it could be used as a surfactant.

2.2.1.1 Quarternization of water-soluble azo-initiator (V-50).

0.061 mol of V-50 (2,2' – Azobis (2-methylpropionamide) dihydrochloride) is dissolved in 2.517 moles of dimethyl formamide (DMF). 0.350 mol of dimethyl sulfate (DMS) is added to the solution, and the mixture has been stirred continuously for 2 h at room temperature. During this period, blurry solution started to be more and more transparent as an indication of the progress of reaction. Treated V-50 (V-50(t)) crystals were precipitated in 1840 g of ethyl acetate. After vacuum drying for 12 h, V-50(t) was stored at -15°C . The progress of reaction was characterized by Nuclear Magnetic Resonance Spectroscopy $^1\text{H-NMR}$ (Varian 500 MHz NMR) and Differential Scanning Calorimetry-DSC (Netzsch DSC 204, Selb, Germany) between $30\text{-}350^\circ\text{C}$ under nitrogen atmosphere.

2.2.1.2 Na^+ -MMT Treatment and characterization

Na^+ -MMT was ion exchanged with first three different surfactants industrially used; Tequart DSM, BTC 1218-50. Then under the guidance of WAXD data in terms of the efficiency of surfactants, six different combinations of Tequart DSM, BTC 1218-50 and V-50(t) has been used as modifier. Their combinations were arranged to obtain an organophilic MMT and have been summarized in Table 2.1 and labeled with increasing

numbers of modified clay (MC) . Amount of each surfactant or surfactant-(V-50(t)) combination was calculated in such a way that surfactant in the system is twice as much as the CEC of Na⁺-MMT. A standard procedure for clay treatment [53] (Fig. 2.1) has been performed with 42 grams of Na⁺-MMT dissolved in 1358 grams of distilled water, and calculated amount of surfactant according to active ingredient at 80°C for 19h. while the solution was being continuously stirred.

Table 2.1 Table of clay modifier contents.

Clay #	Tequant DSM (mol)	BTC (mol)	V-50 (mol)	V-50(t) (mol)	MMT (g)
MC-1	0.0483	--	--	0.0483	42
MC-2	--	0.0483	0.0483	--	42
MC-3	--	0.0966	--	--	42
MC-4	--	0.0483	--	0.0483	42
MC-5	0.0966	--	--	--	42
MC-6	0.0483	--	0.0483	--	42

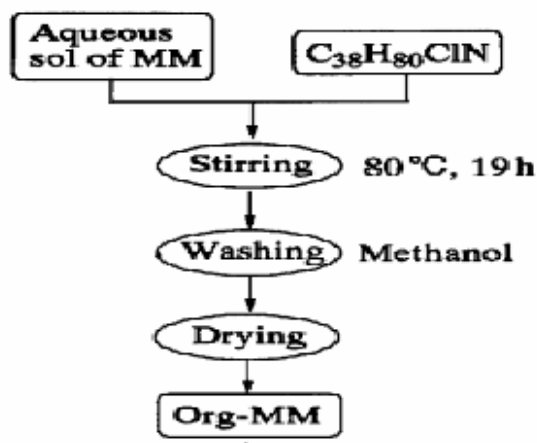


Fig. 2.1 Clay treatment procedure.[53]

Finally, clay was isolated from the solution by filtration and washed with 300 ml methanol twice to get rid of unreacted species. Samples are then dried in vacuum oven for 2 hours. Efficiency of surfactants were tested by X-ray diffractometer (Bruker AXS-D8, Karlsruhe, Germany). The measurements were performed in the 2θ range of 2°-10° at 40 kV and 40 mA. In all measurements, the step size was 0.03°, and data collection period was

2 seconds in each step. Thermo Gravimetric Analysis was also realized to investigate the amount of surfactant located within the clay galleries with a Netzsch STA 449C Jupiter between 30 -600 °C under Nitrogen atmosphere and between 600-800 °C under Oxygen media.

2.2.2 Nanocomposite preparation and characterization.

Organo-philic MMTs, MC-1 and MC-5 were polymerized through bulk polymerization with styrene to make nanocomposite masterbatches. Styrene used was purified through fractional vacuum distillation. Clay: styrene weight ratio was 1:3. For the MC-5 containing polymerization set up, additional V-50_(t) was used to initiate polymerization. Polymerization process was done under N₂ atmosphere at 55 °C for 24 h. The products were precipitated in 1000 ml methanol and dried in vacuum oven at 50 °C for 4 hours. MC-1, MC-5 and their polymerized forms (masterbatches) were then melt blended with standard SEBS grade at compositions where clay concentration was wt. 2.25 % , 5 % and total batch weight was 250 grams with a Thermo Haake Rheomix 3000P internal mixer at 200 °C and 120 rpm for 6 minutes. MC 1 was also melt blended with SEBS-MA and standard SEBS compound mixture where SEBS-MA content of the blend was at least twice as much as clay content in the final nanocomposites. Samples for testing were prepared by carrying hot-melt to a compression mold at 200 °C.

At the end, we had blends of MC1, MC5, MC1 and MC5 polymerized in styrene (MC1-MB, and MC5-MB respectively) and MC1 in SEBS-MA (wt. %10) and SEBS blend. Tensile testing was done with an industrial Zwick Z020 and x-ray diffractometer used for clay characterization in upper section was also run for characterization of nanocomposites with exactly the same method. Scanning Electron Microscope (SEM) images of nanocomposites were obtained by a Leo Supra 35 VP. All samples are exposed to liquid nitrogen for three minutes and fractured surfaces were examined in order to investigate the dispersed modified clays. Surfaces were coated with approximately 30 nanometers layer of gold with plasma deposition technique. Both inlens and backscattered electron detectors were used for morphologic analysis. SEM images are presented with WAXD patterns that

indicate the degree of delamination within clay galleries and the conditions that images are taken are presented at the bottom of each piece.

CHAPTER 3

RESULTS AND DISCUSSION

3.1. Novel idea for PCN preparation

In this thesis, we combined melt intercalation method and in-situ intercalative polymerization method for producing SEBS/Clay nanocomposite. In such a challenge, first the most appropriate clay type, second surfactant for clay treatment, and finally methods for nanocomposite preparation have been investigated.

As the most suitable clay type for modification, Na⁺-MMT with the most suitable cation exchange capacity (CEC=110 meq/100g) and particle length (100-150 nm) pair among the clay types has been chosen. Two types of surfactants which are readily available and serve for detergent industry in softener formulations have been used; N-N dialkyl dimethyl ammonium chloride (**Tequart DSM**) and Alkyl dimethyl benzyl ammonium chloride (**BTC 1218-50**). They have been used for their ability to exchange with Na⁺ located in the interlayer spacing of MMT. Their efficiency in intercalating the clay galleries have been investigated via WAXD patterns.[12,18,40,41]

The novel application used was combination of two techniques used for PCN preparation. We have been inspired by the idea Toyota Research Group used for N6/Clay nanocomposites; intercalative polymerization technique. They first reported the ability of a

, α -amino acids ($\text{COOH}-(\text{CH}_2)_{n-1}-\text{NH}_2^+$, with $n = 2; 3, 4, 5, 6, 8, 11, 12, 18$) modified Na^+ -MMT to be swollen by the ϵ -caprolactam monomer. at 100°C and subsequently initiate its ring opening polymerization to obtain N6/MMT nanocomposites.[35] In this case, α -amino acid was a logical choice since it can guarantee the progress of polymerization within clay galleries so growing oligomer chains cause an increase in basal spacing of clay. But this case is unique for Nylon 6 and not applicable to all kind of monomers. As an alternative way, Pantoustier et al. [39] prepared a solution of initiator and added to reaction vessel at the desired time to begin polymerization. Here, another problem arises because of the location of polymerization initiation. Polymerization can take place anywhere in reaction media and possibility of oligomers intercalating the clay decreases.

What is novel in our study was incorporation of a modified initiator that will both initiate the polymerization, and behave as a surfactant and locate within clay galleries like in the case of α -amino acids in PCL nanocomposites. We have quarternized 2,2'-Azobis(2-methyl propionamide) (Fig. 1.21), a water soluble initiator with Dimethylsulfate. Nitrogen atoms in both ends of the initiator molecule lost Hydrogen atoms attached to them and are positively charged. This water soluble quarternized initiator would tend to exchange with Na^+ ions. Initiator was used with surfactant in equal compositions in order to realize this idea. Some excess amount was used to eliminate the efficiency loss caused by half life of initiator.

The second step was to polymerize a suitable monomer that will be compatible with SEBS; melt intercalation method. MMT that was modified by the novel idea was added to styrene monomer and mixture was bulk polymerized. The product would be a nanocomposite masterbatch that will be compatible with the polystyrene domains (Fig.1.2) in SEBS. Then these masterbatches were melt mixed with SEBS in varying weight percentages. Classical attempt was also applied that MMT modified with only surfactant melt mixed with SEBS. Final method tested was incorporation of maleic anhydride grafted polymer in melt mixing process like Usuki et al. [45] had reported. They thought that OH groups in maleic anhydride could react with Oxygen atoms in MMT structure which would make intercalation of polymer chains into spacings easier.

3.2 Clay Treatment

Before discussing on the efficiency of surfactants used in this study one has to consider the success of the reaction that makes the initiator a quarternized azo compound and so it would behave as an organic modifier and surfactant for Na-montmorillonite. Methylation of water-soluble azo-initiator; 2,2'-Azobis(2-methyl propionamide) (Fig.1.21) was proceeded by $^1\text{H-NMR}$ and DSC study. Reaction with dimethylsulfate caused Nitrogen atoms in both ends of the initiator molecule to lose Hydrogen atoms attached to them. After reaction two new peaks at 2.65 ppm and 3.9 ppm for initiator arised in $^1\text{H-NMR}$ spectrum. (Fig. 3.1.)

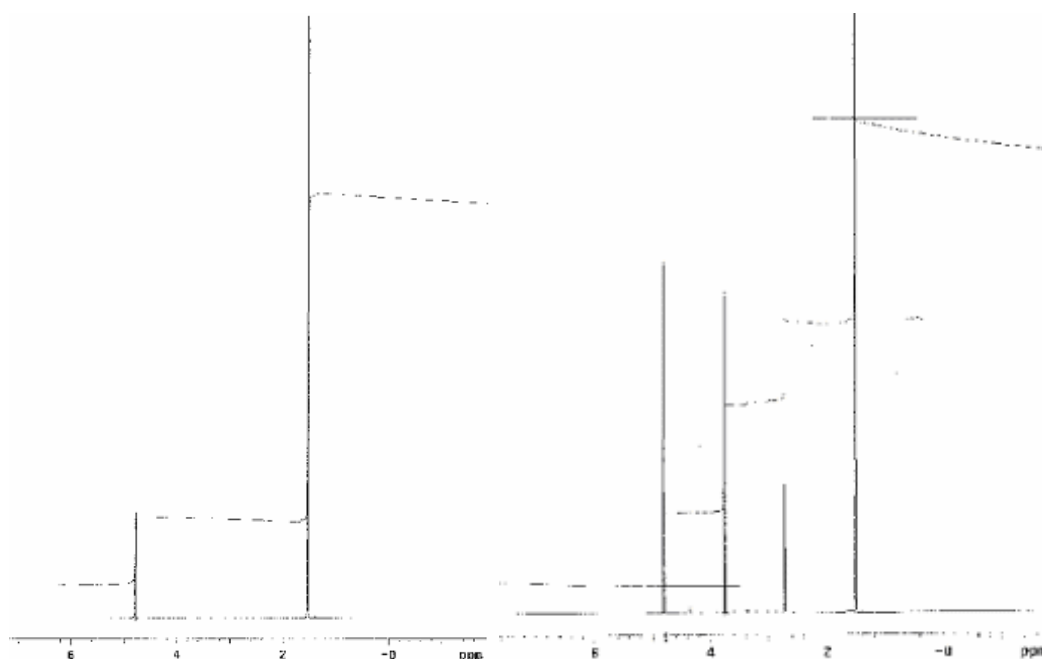


Fig. 3.1 $^1\text{H-NMR}$ spectra of water soluble azo-initiator before (left) and after (right) quarternization with dimethylsulfate.

The higher peak in the spectrum of untreated initiator belongs to hydrogen atoms in methyl groups and there are 12 hydrogens. The two new peaks rising represents at most four new

methyl groups donated by dimethylsulfate to the structure. We can conclude that the reaction caused a modification as we required and methylation improves ionic character. WAXD pattern evaluation also supported this result and treated initiator surfactant pair contributed to increasing interlayer spacings of clay.

DSC thermograms show that melting peak of untreated initiator at 173.9 °C shifts to 119.5 °C after quarternization reaction. (Fig 3.2.) This was revealing that the reaction formed a thermally less stable compound but also indicating the success of treatment together with NMR data. A broader peak was because of imperfect crystallization of treated initiator solution.

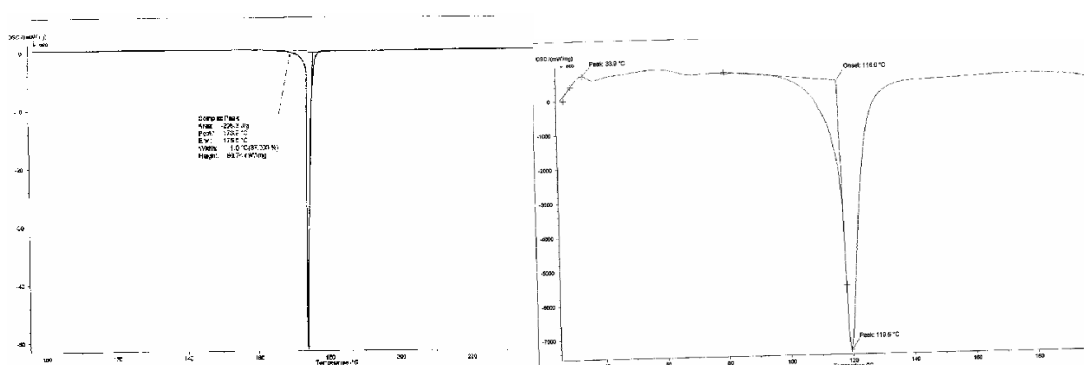


Fig. 3.2. DSC thermogram of water soluble azo -initiator before (left) and after (right) quarternization with dimethylsulfide.

Na⁺ -MMT treatment was done with first three surfactants and then with various initiator-surfactant pairs and surfactants (Table 2.1) according to the method explained in Fig 2.1. [53] Through the route to most efficient surfactant selection WAXD patterns were compared. By monitoring the position, shape, and intensity of the basal reflections from the distributed silicate layers, the nanocomposite structure (intercalated or exfoliated) was identified. [5] According to Bragg's Law ($2d\sin\theta = n\lambda$), interlayer spacing of the galleries is inversely proportional with the sine of the angle of reflected x-ray beam (θ) so as the peaks on WAXD patterns approach to very small angles then basal spacings inevitably increase. If lamellar structure is destroyed and clay layers lose their orientation (exfoliation) there are no more peaks to observe. Based on this idea, Tequart DSM clearly manages the maximum delamination within surfactants. Basal spacing of Na⁺-MMT treated with Tequart DSM reaches up to the value of 1.9 nm which was 1.2 nm for pristine clay.

On the other hand, BTC 1218-50 was also successful that the value for it was about 1.4 nm. Tequart DSM has managed to delaminate more than Cloisite 15 A (1.38 nm) whereas BTC 1218-50 had almost same 2θ value but the peak for Cloisite 15 A was much more intense than those of two surfactants. More intense peak means that a larger portion of the clay particles have been reached to that specific interlayer distance. So it can be concluded that in commercial grade intercalation of surfactant molecules have been achieved for a higher percentage of clay particles with same efficiency. For Viscobent, another commercial grade, the case was a little bit different because of the quality of clay. There were two peaks close to each other one was at a smaller 2θ value than BTC 1218-50 (1.68 nm) and one at a higher value (1.24 nm). This could be because of mixing of different kinds of clay used for treatment. We have briefly observed that both of the surfactants with the help of method used were more successful than commercial grades but Tequart DSM had a more intense peak. In other words, more clay particles had been treated.

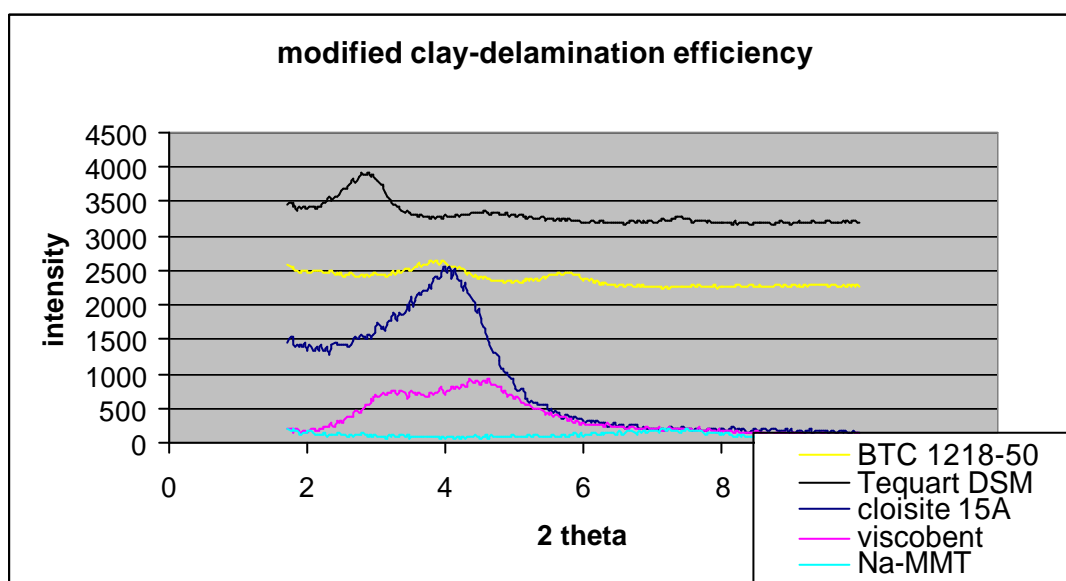


Fig.3.3 Comparison of WAXD patterns of treated clays and commercial grades.

Thermogravimetric Analysis of these treated clays also confirmed these result.(Fig 3.4) Weight loss after heating up to 800 °C where all organic surfactant molecules decomposes revealed us more Tequart DSM molecules has penetrated within the galleries. Weight percent of Tequart DSM and BTC 1218-50 in the clay were 36.05 and 26.76

respectively. Tequart DSM was also more thermally stable since it had started to lose weight at a higher temperature.

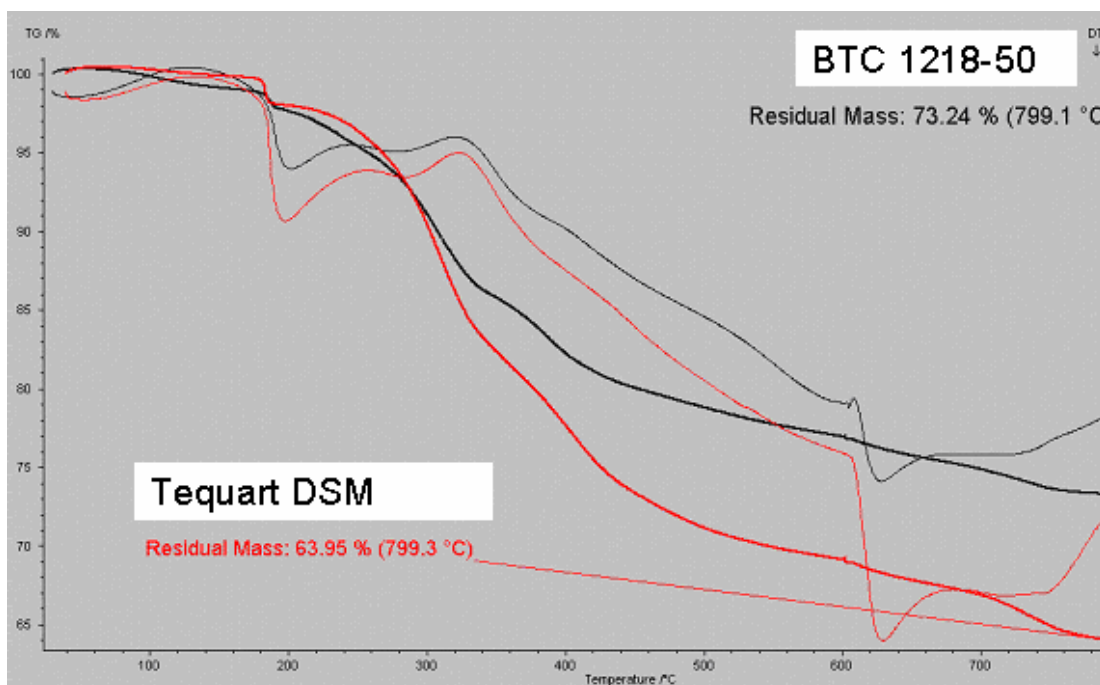


Fig. 3.4 Thermogravimetric Analysis of Na⁺-MMT treated with two surfactants.

The second step of the study was to go further in terms of intercalation and try efficiency of various surfactant-initiator and surfactant-treated initiator pairs. (Table 2.1) We have questioned whether our treated initiator, which has positively charged Nitrogen atoms in its structure, will contribute intercalation efficiency or not. Some increase in basal spacing would mean that initiator molecules had located within galleries so polymerization could start exactly at the right place. Formation of oligomers; growing chains in between layers would cause to increase spacing and disturb crystal structure. When the polymerization builds up a considerable pressure, exfoliation could be achieved.

WAXD patterns confirmed our thoughts that even untreated initiator-surfactant pairs helped delamination. Tequart DSM-treated V-50 (MC1) succeeded the most delamination (2.35 nm) at the smallest 2θ angle. Modification efficiency results with the other compositions can be summarized as: Tequart DSM-untreated V-50 (MC6) to 2.02 nm, BTC 1218-50-treated V-50 (MC4) to 1.07 nm, and BTC 1218-50-untreated V-50

(MC2) to 1.07 nm. (Fig 3.5) Both of the surfactants are applied alone for control purposes and satisfying the results of first set of experiments. Initiator modification led to an extra 0.28 nm increase in basal spacing for Tequart DSM- V-50 pair but had no effect in the case of BTC 1218-50-V50 pair. The reason of these phenomena is out of focus of this thesis but an interesting result that should be explained in a deeper research on this subject. It was even worse than BTC 1218-50 alone and told us that BTC 1218-50 was not suitable for the rest of the study where we want to challenge the most suitable and efficient combination. When intensities were considered, one might observe that MC1 could penetrate to more clay particles. This result was also satisfying our approach on MC1 to be the best combination for the next set of experiments for masterbatch preparation.

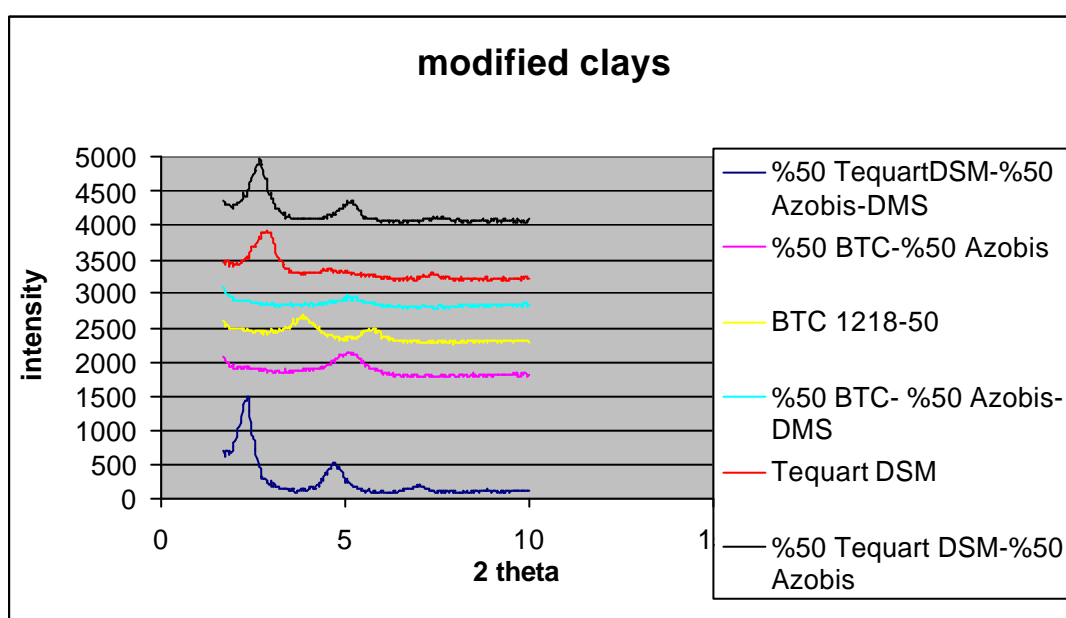


Fig. 3.5 WAXD patterns of surfactant-initiator pairs.

Thermogravimetric analysis supported our idea and Tequart DSM combinations had smaller residual mass when compared with corresponding BTC 1218-50 combination. (Fig. 3.6) Tequart DSM-treated V-50, Tequart DSM-untreated V-50, and Tequart DSM have intercalated % 32.32, % 31.46, and % 36.05 respectively. We expected the treated initiator system to be the most penetrating one. It was better than untreated one but worse than the surfactant only. This is mainly because of huge differences between molecular weights of surfactant and initiator since we considered an equimolar mixture of them. BTC 1218-50

pairs seem to be thermally more stable but their failure in modification made them out of focus.

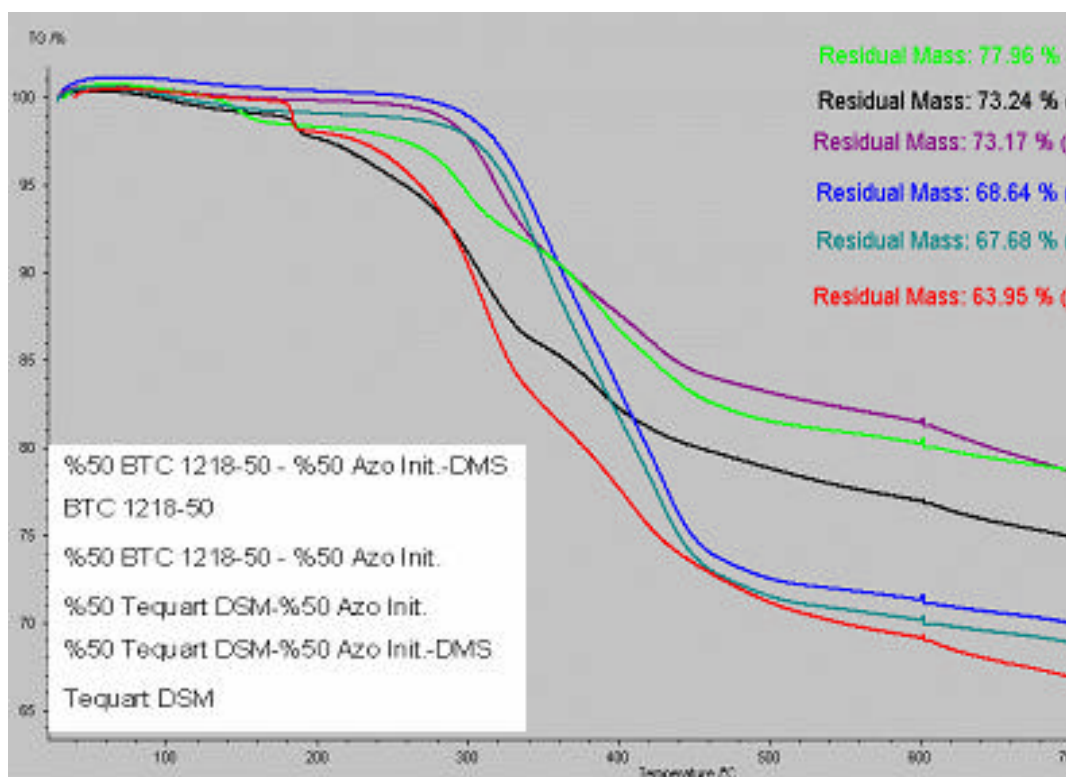


Fig. 3.6 Thermogravimetric Analysis of surfactant-initiator pairs.

3.3. Nanocomposites and their properties

The data above led us to continue the rest of the study with Tequart DSM-treated V-50 with DMS (MC1) modified clay. In this final part of the thesis we have tried several approaches for preparation of nanocomposites of a standard unfilled SEBS grade. Each attempt was melt mixed with SEBS and compression molded plaques were prepared for testing. One of these was directly melt blending MC1 at compositions of 2.25 and 5 weight percent in order to discover the effect of increasing clay content. Another one was a mixture of 10 % Maleic anhydride grafted SEBS (SEBS-MA), 5 % MC1, and 85 % SEBS by weight. This combination was created to see the effect of reaction between Maleic anhydride and clay, which would increase the compatibility and enhance mechanical properties like Usuki et al. proposed. [45] The final approach was the main idea in this

study that polymerization of styrene within clay galleries would result to a masterbatch (25 % weight percent) that was potentially a proper, easy to process polymer additive. This process could also help to achieve a higher degree of intercalation. The final sample was a 20% masterbatch (5 % MC1) melt mixed one.

SEM image of masterbatch (Fig 3.7) gives us a general idea about particle size distribution and success of the polymerization. Clay particles encapsulated with polystyrene can easily be seen in the image. But some agglomerations are also observed. This may be due to irregular particle size distribution of the original clay or just because of the polystyrene matrix that holds clay particles together. If this is the case, during melt mixing these agglomerates should have been destroyed.

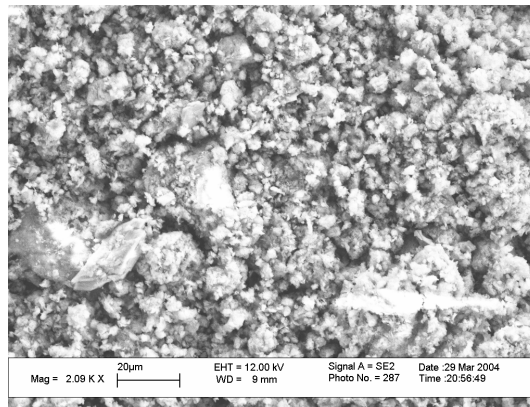


Fig. 3.7 SEM image of MC1-polystyrene masterbatch.

WAXD patterns of blends first of all satisfied our claim that masterbatch preparation through in-situ intercalative polymerization had caused more number of clay particles to be delaminated since this sample has a more intense peak than all others.

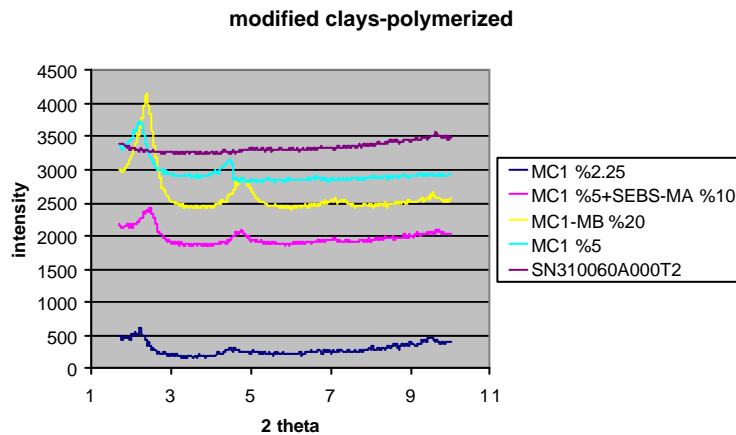


Fig 3.8 WAXD patterns of various melt blends.

Masterbatch preparation increased the efficiency of nanocomposite preparation as well as making the processability easier. Increasing clay content in the matrix from 2.25 % to 5 % also led to the formation of an intenser peak. This is predictable because as the clay content reaches to higher values, there are more particles or agglomerates that can be detected with WAXD. SEBS-MA was incorporated the matrix for just better mechanical properties so there should not have been any change in WAXD pattern when compared with that of MC1 5 % sample as it has announced in Fig. 3.8. Standard SEBS grade had no peak since it had no filler present in its formulation.

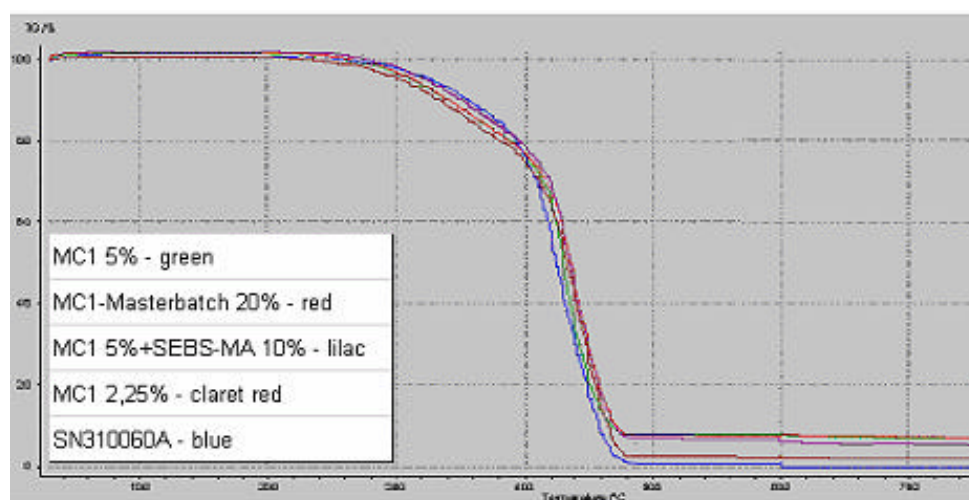


Fig. 3.9 Thermogravimetric analysis of melts blends.

Thermogravimetric analyses were done primarily to satisfy the clay content in each of the blend. In fig. 3.9, it can be seen that 5 % clay compositions have the same residual mass indicating that blends were correctly prepared. SEBS grade has the lowest ash content because it has no filler, and the composition MC1 2.25 % has a residual mass in between them. Another interesting observation comes out of the onset of degradation temperatures. At a close look at, one can see that SEBS grade starts decomposing 15-20 °C indicating that nanocomposites have a better thermal stability than virgin SEBS.

Tensile testing results for nanocomposites are summarized in table 3.1. As it can be easily seen, dispersion of clay to polymer matrix in nano-size rised up the maximum elongation value for all nanocomposites when compared with unfilled SEBS. The case is mostly opposite for micron size fillers. Another interesting result is the decreased tensile strength values which mean that the force required for maximum elongation has decreased.

Briefly material tends to be more elastic with less amount of tensile stress applied as nano dispersion occurs.

Table 3.1. Mechanical properties of nanocomposites

Mechanical properties	Tensile Strength at Break	Elongation at Break	100% Modulus	200% Modulus	300% Modulus
Standard-Unit	ISO 37-Mpa	ISO 37-%	ISO 37-Mpa	ISO 37-Mpa	ISO 37-Mpa
MC1 2,25%	5,41	627,31	1,01	1,46	1,97
MC1 5%+SEBS-MA 10%	5,28	642,87	1,12	1,63	2,17
MC1-Masterbatch 20%	6,76	631,12	1,43	2,10	2,78
MC1 5%	5,21	616,24	1,02	1,45	1,93
SN310060A	6,86	599,03	1,28	1,84	2,47

After this general evaluation about benefits, a closer comparison of results tells us the exact effects of different techniques. When we consider MC1 2,25% and MC1 5%, we see that as the clay content increase even if a nanocomposite forms, maximum elongation value that are 627% and 616,24% respectively decreases. But tensile strength value decreases from 5.28 to 5.21 Mpa. However MC1-MB has some more rigid styrene content contributed from masterbatch, it has a higher elongation at break value than MC1 5% where treated clay is directly melt mixed with co-polymer system. SEBS-MA containing sample has the highest elongation value (642,87%) and it has a tensile strength less than MC1-MB but higher than MC1 %5. Compatibilization through masterbatch preparation or SEBS-MA incorporation which will react with clay consistently rised elongation at break values. But masterbatch technique rised also tensile strength which is due to extra styrene addition to matrix. In fact, such an addition may decrease the elongation value but success of compatibilization overcame this negative effect of inorganic filler and extra styrene addition to the system. It has just dropped the elongation at break approximately 11% which is not really important in case where elongation is around 600-650%. Another fact is

that within all nanocomposites, MC1-MB has the closest tensile strength to virgin unfilled material.

SEM imaging also gave us a chance to observe dispersed clay particles and to determine their particle size. First of all, the difference in the morphology of MC1-MB nanocomposite and unfilled SEBS were compared. (Fig. 3.10) The mono-phase surface of SEBS has turned to an interesting pattern full of details and objects. Big and very shiny particles are basically gold particles that have been used for coating. Clay particles are small irregular shaped and semi-immersed projecting parts having particles size between 0.5-4 microns. What is observed is stacked layers together which means that the nanocomposites are intercalative rather than exfoliated in harmony with WAXD patterns. This composition becomes clearer at higher magnifications (Fig. 3.11) Image formed after processing of backscattered electrons presents the dispersion efficiency and general appearance of matrix. Another image taken at 65000 magnifications with inlens detector shows the stacked layers of clay, which are evidence of intercalated nanocomposite structure.

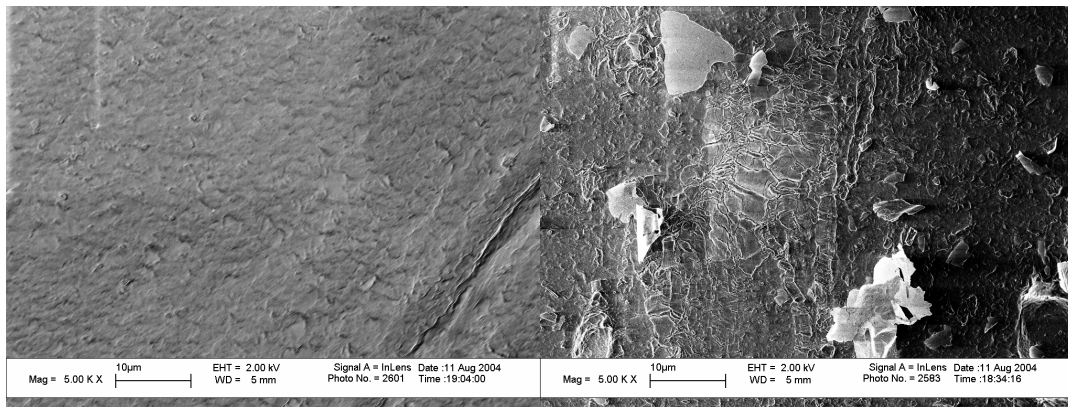


Fig.3.10 SEM image of unfilled SEBS (left) and MC1-MB nanocomposite.

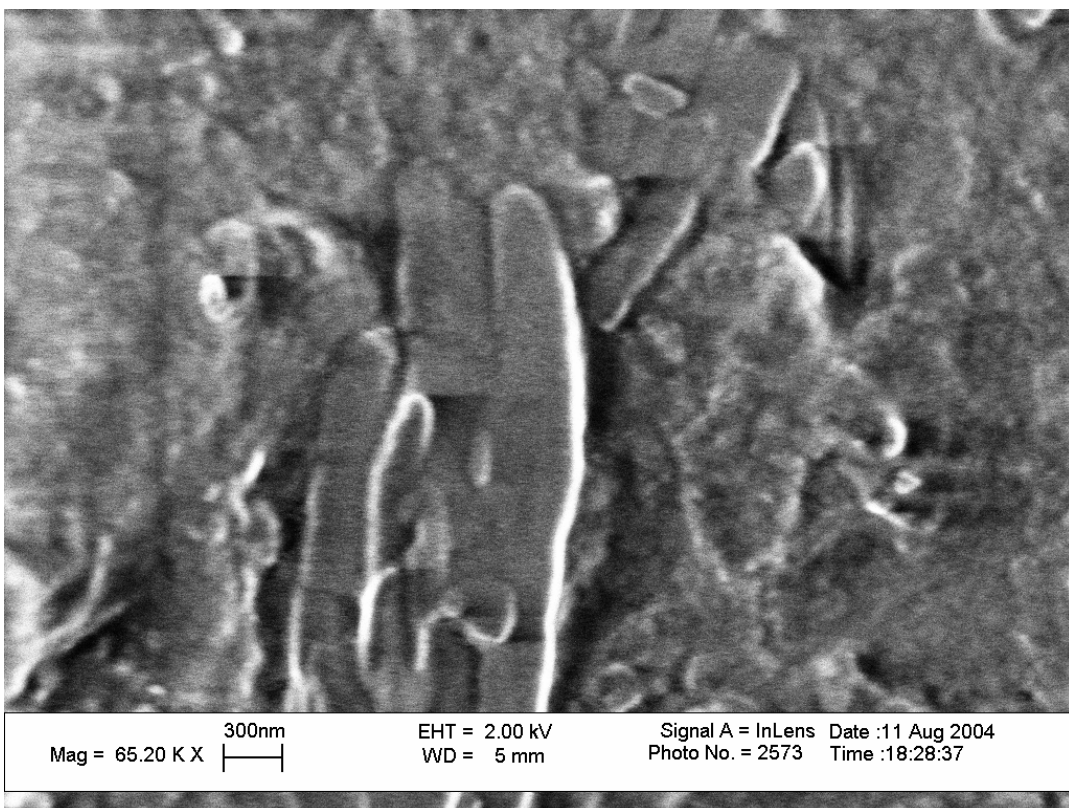
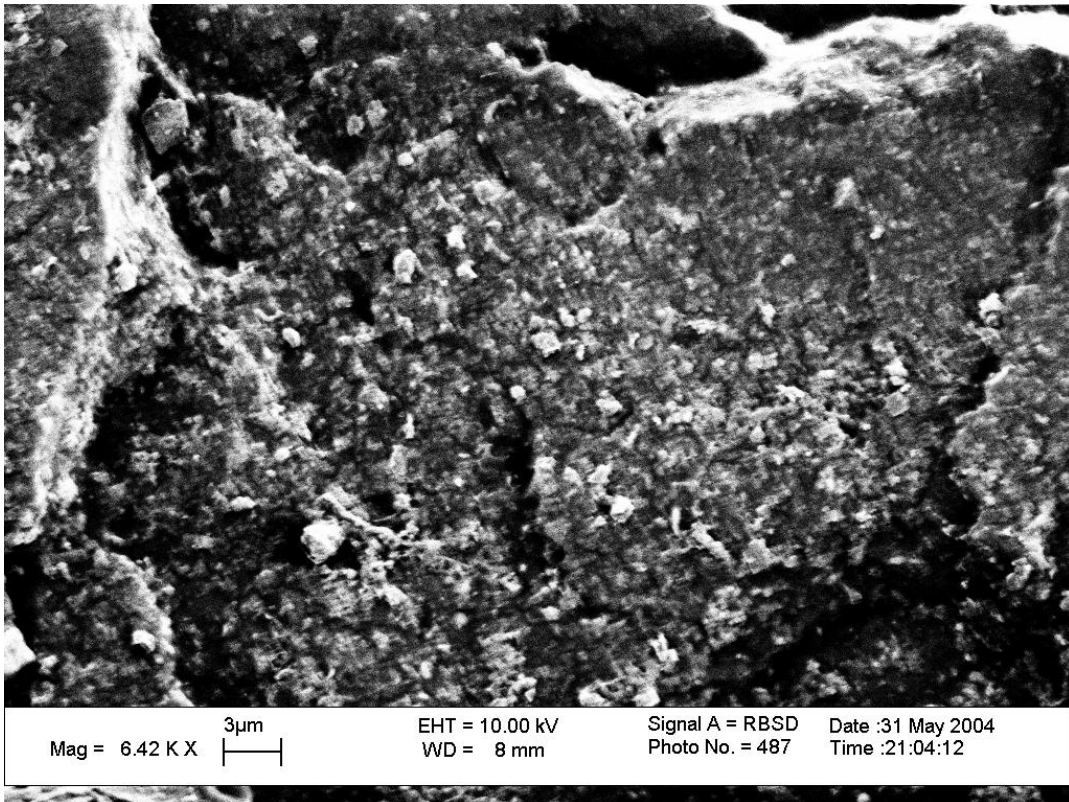


Fig. 3.11 SEM images of MC1-MB nanocomposite at higher magnifications.

CHAPTER 4

CONCLUSIONS

This study aims to successfully synthesize SEBS-clay nanocomposites with enhanced properties but with easy-to-find, cheap ingredients and easiest, most efficient and most commercially viable method. So a research route to find most efficient application has been followed. In this thesis, we combined melt intercalation method and in-situ intercalative polymerization method for producing SEBS/Clay nanocomposite. In such a challenge, the most appropriate clay type, surfactant for clay treatment, method for nanocomposite preparation have been investigated. This study searches the route to economically feasible, industrially applicable, and environmentally friendly way of producing SEBS/Clay nanocomposites.

What is novel in this study was incorporation of a modified initiator in nanocomposite preparation that will behave as a surfactant. The in-situ intercalative polymerization in the presence of best surfactant and initiator pair would result in formation of a masterbatch of modified clays in polystyrene at a nanocomposite structure. Then this masterbatch that was claimed to be compatible with styrene domains in the SEBS structure was melt blended with SEBS and properties have been compared with nanocomposites prepared with other techniques.

We have methylated 2,2'-Azobis(2-methyl propionamide), a water soluble initiator with Dimethylsulfate. Methylation of water soluble azo-initiator; 2,2'-Azobis(2-methyl

propionamide) (Fig.1.21) was proceeded by $^1\text{H-NMR}$ and DSC study. The two new peaks rising in the $^1\text{H-NMR}$ spectrum of treated initiator represents at most four new methyl groups donated by dimethylsulfate to the structure. DSC thermograms show that melting peak of untreated initiator at $173.9\text{ }^\circ\text{C}$ shifts to $119.5\text{ }^\circ\text{C}$ after quaternization reaction.

Second, best surfactant that can be used for clay modification has been chosen based on WAXD analysis. Interlayer spacings of Na^+ -MMT treated with different surfactants have been calculated by Braggs Law. Basal spacing of Na^+ -MMT treated with Tequart DSM (N-N dialkyl dimethyl ammonium chloride) reaches up to the value of 1.9 nm which was 1.2 nm for pristine clay. BTC 1218-50 (Alkyl dimethyl benzyl ammonium chloride) was also succesful that the value for it was about 1.4 nm. Tequart DSM has managed to delaminate more than Cloisite 15 A (1.38 nm). Thermogravimetric Analysis of these treated clays also confirmed these result. Weight percent of Tequart DSM and BTC 1218-50 in the clay were 36.05 and 26.76 respectively. Tequart DSM was able to penetrate within layers more and it was also more thermally stable since it had started to lose weight at a higher temperature.

Then best surfactant-modified initiator pair has been investigated. Tequart DSM-treated V-50 (MC1) succeeded the most delamination (2.35 nm) at the smallest 2θ angle. Modification efficiency results with the other compositions can be summarized as: Tequart DSM-untreated V-50 (MC6) to 2.02 nm, BTC 1218-50-treated V-50 (MC4) to 1.07 nm, and BTC 1218-50-untreated V-50 (MC2) to 1.07 nm.

Final part of the thesis tests several approaches for preparation of nanocomposites of a standart unfilled SEBS grade. Each attempt was melt mixed with SEBS and compression molded plaques were tested. Thermogravimetric analysis was done primarily to satisfy the clay content in each of the blend. Tensile testing has shown that dispersion of clay to polymer matrix in nano-size rose up the maximum elongation value for all nanocomposites when compared with unfilled SEBS. Another interesting result is the decreased tensile strength values which mean that the force required for maximum elongation has decreased. Briefly material tends to be more elastic with less amount of tensile stress applied as nano dispersion occurs. As the clay content increase maximum elongation value decreases. Maleic Anhydride grafted SEBS containing sample has the highest elongation value (642,87 %). However our attitude, MC1 masterbatch (MC1-MB),

has some more rigid styrene content contributed from oligomers, it has a higher elongation at break value than MC1 5% where treated clay is directly melt mixed with co-polymer system. Compatibilization through masterbatch preparation or SEBS-MA incorporation which will react with clay consistently rose elongation at break values. But masterbatch technique rose also tensile strength which is due to extra styrene addition to matrix. SEM images in coherence with WAXD data proved that the nanocomposite produced was intercalative.

Further research can be conducted on a more detailed study about surfactant preference, or monomers to be polymerized for other kinds of polymer matrix systems. This application can also be tested for gas barrier properties where a considerable improvement is expected. The most interesting approach will be investigating the fire retardancy improvement contributed from dispersed clays which is mainly because of hugely increased surface area of clays facing with fire. They will cause a synergistic effect when used with traditional flame retardants (FR) and decrease the amount of FR to be used for a specific amount of flame retardancy desired.

REFERENCES

1. Holden G, Legge N.R., "Thermoplastic Elastomers", 2nd Edition, Hanser, USA, 1996.
2. http://www.the-infoshop.com/study/fd10165_thermoplastic_elastomers.html
3. Holden G, Milkovich R., U.S. Patent; 3, 265, 765, 1964.
4. Foreman L.E., "Polymer Chemistry of Synthetic Elastomers", John Wiley and Sons, New York, 1969.
5. Biswas M, Sinha Ray S., "Recent progress in synthesis and evaluation of polymer-montmorillonite nanocomposites" Adv. Polym. Sci; 155, 167–221, 2001.
6. Morton M, "Anionic Polymerization: Principles and Practice", Academic Press, New York, 1983.
7. Dreyfuss P, Fetters L.J., "Rubber Chem. Technol." ,Hanser, USA, 1983.
8. Giannelis E.P., "Polymer-layered silicate nanocomposites: synthesis, properties and applications." Appl. Organomet. Chem.; 12, 675–80, 1998.
9. Xu R, Manias E, Snyder A.J, Runt J., "New biomedical poly(urethane urea)-layered silicate nanocomposites" Macromolecules; 34, 337–9, 2001.
10. Gilman J.W, Jackson C.L, Morgan A.B, Harris Jr.R, Manias E, Giannelis E.P, Wuthenow M, Hilton D, Phillips S.H., "Flammability properties of polymer-layered silicate nanocomposites. Propylene and polystyrene nanocomposites." Chem. Mater.;12, 1866–73, 2000
11. Sinha Ray S, Yamada K, Okamoto M, Ueda K., "New polylactide/layered silicate nanocomposite: a novel biodegradable material." Nano Lett.; 2, 1093–6., 2002.

12. Theng B.K.G., "Formation and properties of clay-polymer complexes." Amsterdam: Elsevier; 1979.
13. Okada A, Kawasumi M, Usuki A, Kojima Y, Kurauchi T, Kamigaito O., "Synthesis and properties of nylon-6/clay hybrids." In: Schaefer DW, Mark JE, editors. Polymer based molecular composites. MRS Symposium Proceedings, Pittsburgh; vol. 171, p. 45-50, 1990.
14. Vaia R.A, Ishii H, Giannelis EP., "Synthesis and properties of two-dimensional nanostructures by direct intercalation of polymer melts in layered silicates." *Chem. Mater.*; 5, 1694-6, 1993.
15. Brindly SW, Brown G, "Crystal structure of clay minerals and their X-ray diffraction." London: Mineralogical Society; 1980.
16. Aranda P, Ruiz-Hitzky E., "Poly(ethylene oxide)-silicate intercalation materials." *Chem. Mater.*; 4, 1395-403, 1992.
17. Greenland DJ., "Adsorption of poly(vinyl alcohols) by montmorillonite." *J. Colloid. Sci.*; 18, 647-64, 1963.
18. Krishnamoorti, Vaia RA, Giannelis E.P., "Structure and dynamics of polymer-layered silicate nanocomposites." *Chem. Mater.*; 8, 1728-34, 1996.
19. Lagaly G., "Interaction of alkylamines with different types of layered compounds." *Solid State Ionics*; 22, 43-51, 1986.
20. Sinha Ray S, Okamoto K, Okamoto M., "Structure-property relationship in biodegradable poly(butylene succinate)/layered silicate nanocomposites." *Macromolecules*; 36, 2355-67, 2003.
21. Vaia R.A, Jant K.D, Kramer E.J, Giannelis E.P., "Microstructural evaluation of melt-intercalated polymer-organically modified layered silicate nanocomposites." *Chem. Mater.*; 8, 2628-35, 1996.
22. Zhiqi Shen, George P. Simon, "Comparison of solution intercalation and melt intercalation of polymer-clay nanocomposites", *Polymer*; 43, 4251-4260, 2002.
23. Lim S, Hyun Y.H, Choi H.J, Jhan M.S., "Synthetic biodegradable aliphatic polyester/montmorillonite nanocomposites." *Chem. Mater.*; 14, 18-44, 2002.
24. Aranda P, Ruiz-Hitzky E., "Poly(ethylene oxide)-silicate intercalation materials." *Chem. Mater.*; 4, 1395-403, 1992.

25. Greenland D.J., "Adsorption of poly(vinyl alcohols) by montmorillonite." *J. Colloid. Sci.*;18, 647–64, 1963.
26. Francis CW., "Adsorption of polyvinylpyrrolidone on reference clay minerals." *Soil. Sci.*; 115, 40–54, 1973.
27. Jimenez G, Ogata N, Kawai H, Ogihara T., "Structure and thermal/mechanical properties of poly(1 -caprolactone)–clay blend." *J. Appl. Polym. Sci.*; 64, 2211–20, 1997.
28. Ogata N, Jimenez G, Kawai H, Ogihara T. "Structure and thermal/mechanical properties of poly(L-lactide)–clay blend." *J. Polym. Sci., Part B: Polym Phys*; 35, 389–96, 1997.
29. Jeon HG, Jung HT, Lee SW, Hudson SD., "Morphology of polymer silicate nanocomposites. High density polyethylene and a nitrile." *Polym. Bull.*; 41, 107–13, 1998.
30. Kawasumi M, Hasegawa N, Usuki A, Okada A., "Nematic liquid crystal/clay mineral composites." *Mater. Sci. Engng. C*; 6, 135–43,1998.
31. Vaia RA, Giannelis EP., "Lattice of polymer melt intercalation in organically-modified layered silicates. *Macromolecules*; 30, 7990–9, 1997.
32. Wu J, Lerner M.M., "Structural, thermal, and electrical characterization of layered nanocomposites derived from sodium-montmorillonite and polyethers." *Chem. Mater.*; 5, 835–8, 1993.
33. Burnside S.D, Giannelis E.P., "Synthesis and properties of new poly (dimethylsiloxane) nanocomposites. *Chem. Mater.*; 7, 1597–600, 1995.
34. Yano K, Usuki A, Okada A. "Synthesis and properties of polyimide–clay hybrid films." *J. Polym. Sci., Part A: Polym Chem.*; 35, 2289–94, 1997.
35. Usuki A, Kawasumi M, Kojima Y, Okada A, Kurauchi T, Kamigaito O., "Swelling behavior of montmorillonite cation exchanged for α -amine acid by ϵ -caprolactam." *J. Mater. Res.*; 8, 1174–8, 1993.
36. Messersmith PB, Giannelis EP., "Polymer-layered silicate nanocomposites: in-situ intercalative polymerization of 1 - caprolactone in layered silicates." *Chem Mater*; 5, 1064–6, 1993.

37. Messersmith P.B, Giannelis E.P., “Synthesis and barrier properties of poly(1 -caprolactone)-layered silicate nanocomposites.” *J. Polym. Sci., Part A: Polym. Chem.*; 33, 1047–57, 1995.
38. Chen T.K, Tien Y.I, Wei K.H., “Synthesis and characterization of novel segmented polyurethane/clay nanocomposite via poly(1 -caprolactone)/clay.” *J. Polym. Sci., Part A: Polym. Chem.*; 37, 2225–33, 1999.
39. Okamoto M, Morita S, Taguchi H, Kim Y.H, Kotaka T, Tateyama H. “Synthesis and structure of smectic clay/ poly(methyl methacrylate) and clay polystyrene nanocomposites via in situ intercalative polymerization.” *Polymer*; 41, 3887–90, 2000.
40. Okamoto M, Morita S, Kotaka T., “Dispersed structure and ionic conductivity of smectic clay/polymer nanocomposites.” *Polymer*; 42, 2685–8, 2001.
41. Vaia R.A, Giannelis E.P., “Polymer melts intercalation in organically-modified layered silicates: model predictions and experiment.” *Macromolecules*; 30, 8000–9, 1997.
42. Beyer F.L, Tan N.C.B, Dasgupta A, Galvin M.E., “Polymerlayered silicate nanocomposites from model surfactants.” *Chem Mater*; 14, 2983–8, 2002.
43. Usuki A, Kato M, Okada A, Kurauchi T. “Synthesis of polypropylene–clay hybrid.” *J. Appl. Polym. Sci.*; 63, 137–8, 1997.
44. Kawasumi M, Hasegawa N, Kato M, Usuki A, Okada A. “Preparation and mechanical properties of polypropylene–clay hybrids.” *Macromolecules*; 30, 6333–8, 1997.
45. Hasegawa N, Kawasumi M, Kato M, Usuki A, Okada A., “Preparation and mechanical properties of polypropylene –clay hybrids using a maleic anhydride-modified polypropylene oligomer.” *J. Appl. Polym. Sci.*; 67, 87–92, 1998.
46. Pantoustier N, Alexandre M, Degee P, Calberg C, Jerome R, Henrist C, Cloots R, Rulmont A, Dubois P., “Poly(1-caprolactone) layered silicate nanocomposites: effect of clay surface modifiers on the melt intercalation process.” *e-Polymer*; 9,1–9, 2001.

47. Nam P.H, Maiti P, Okamoto M, Kotaka T, Hasegawa N, Usuki A., "A hierarchical structure and properties of intercalated polypropylene/clay nanocomposites." *Polymer*; 42, 9633–40, 2001.
48. Manias E., "A direct-blending approach for polypropylene/ clay nanocomposites enhances properties." *Mater. Res. Soc. Bull.*; 26, 862–3, 2001.
49. Zhu J, Morgan A.B, Lamelas F.J, Wilkie C.A., "Fire properties of polystyrene–clay nanocomposites." *Chem. Mater.*; 13, 3774–80, 2001.
50. Yano K, Usuki A, Okada A, Kurauchi T, Kamigaito O., "Synthesis and properties of polyimide–clay hybrid." *J. Polym. Sci., Part A: Polym Chem*; 31, 2493–8, 1993.
51. Nam P.H, Maiti P, Okamoto M, Kotaka T., "Foam processing and cellular structure of polypropylene/clay nanocomposites." *Proceeding Nanocomposites*, June 25–27, 2001, Chicago, Illinois, USA: ECM Publication; 2001.
52. Strawhecker K.E, Manias E., "Structure and properties of poly(vinyl alcohol)/NaS-montmorillonite nanocomposites." *Chem. Mater*; 12, 2943–9, 2000.
53. Pinnavaia T.J, Beall G.W, "Polymer-Clay Nanocomposites", John Wiley and Sons, England, 150-155, 2000.

REFERENCES

1. Holden G, Legge N.R., "Thermoplastic Elastomers", 2nd Edition, Hanser, USA, 1996.
2. http://www.the-infoshop.com/study/fd10165_thermoplastic_elastomers.html
3. Holden G, Milkovich R., U.S. Patent; 3, 265, 765, 1964.
4. Foreman L.E., "Polymer Chemistry of Synthetic Elastomers", John Wiley and Sons, New York, 1969.
5. Biswas M, Sinha Ray S., "Recent progress in synthesis and evaluation of polymer-montmorillonite nanocomposites" Adv. Polym. Sci; 155, 167–221, 2001.
6. Morton M, "Anionic Polymerization: Principles and Practice", Academic Press, New York, 1983.
7. Dreyfuss P, Fetters L.J., "Rubber Chem. Technol." ,Hanser, USA, 1983.
8. Giannelis E.P., "Polymer-layered silicate nanocomposites: synthesis, properties and applications." Appl. Organomet. Chem.; 12, 675–80, 1998.
9. Xu R, Manias E, Snyder A.J, Runt J., "New biomedical poly(urethane urea)-layered silicate nanocomposites" Macromolecules; 34, 337–9, 2001.
10. Gilman J.W, Jackson C.L, Morgan A.B, Harris Jr.R, Manias E, Giannelis E.P, Wuthenow M, Hilton D, Phillips S.H., "Flammability properties of polymer-layered silicate nanocomposites. Propylene and polystyrene nanocomposites." Chem. Mater.;12, 1866–73, 2000
11. Sinha Ray S, Yamada K, Okamoto M, Ueda K., "New polylactide/layered silicate nanocomposite: a novel biodegradable material." Nano Lett.; 2, 1093–6., 2002.

12. Theng B.K.G., "Formation and properties of clay-polymer complexes." Amsterdam: Elsevier; 1979.
13. Okada A, Kawasumi M, Usuki A, Kojima Y, Kurauchi T, Kamigaito O., "Synthesis and properties of nylon-6/clay hybrids." In: Schaefer DW, Mark JE, editors. Polymer based molecular composites. MRS Symposium Proceedings, Pittsburgh; vol. 171, p. 45-50, 1990.
14. Vaia R.A, Ishii H, Giannelis EP., "Synthesis and properties of two-dimensional nanostructures by direct intercalation of polymer melts in layered silicates." Chem. Mater.; 5, 1694-6,1993.
15. Brindly SW, Brown G, "Crystal structure of clay minerals and their X-ray diffraction." London: Mineralogical Society; 1980.
16. Aranda P, Ruiz-Hitzky E., "Poly(ethylene oxide)-silicate intercalation materials." Chem. Mater; 4,1395-403, 1992.
17. Greenland DJ., "Adsorption of poly(vinyl alcohols) by montmorillonite." J. Colloid. Sci.; 18, 647-64, 1963.
18. Krishnamoorti, Vaia RA, Giannelis E.P., "Structure and dynamics of polymer-layered silicate nanocomposites." Chem. Mater.; 8, 1728-34, 1996.
19. Lagaly G., "Interaction of alkylamines with different types of layered compounds." Solid State Ionics; 22, 43-51, 1986.
20. Sinha Ray S, Okamoto K, Okamoto M., "Structure-property relationship in biodegradable poly(butylene succinate)/layered silicate nanocomposites." Macromolecules; 36, 2355-67, 2003.
21. Vaia R.A, Jant K.D, Kramer E.J, Giannelis E.P., "Microstructural evaluation of melt-intercalated polymer-organically modified layered silicate nanocomposites." Chem. Mater.; 8, 2628-35, 1996.
22. Zhiqi Shen, George P. Simon, "Comparison of solution intercalation and melt intercalation of polymer-clay nanocomposites", Polymer; 43,4251-4260, 2002.
23. Lim S, Hyun Y.H, Choi H.J, Jhan M.S., "Synthetic biodegradable aliphatic polyester/montmorillonite nanocomposites." Chem. Mater.; 14, 18-44, 2002.
24. Aranda P, Ruiz-Hitzky E., "Poly(ethylene oxide)-silicate intercalation materials." Chem. Mater.; 4, 1395-403, 1992.

25. Greenland D.J., "Adsorption of poly(vinyl alcohols) by montmorillonite." *J. Colloid. Sci.*;18, 647–64, 1963.
26. Francis CW., "Adsorption of polyvinylpyrrolidone on reference clay minerals." *Soil. Sci.*; 115, 40–54, 1973.
27. Jimenez G, Ogata N, Kawai H, Ogihara T., "Structure and thermal/mechanical properties of poly(1 -caprolactone)–clay blend." *J. Appl. Polym. Sci.*; 64, 2211–20, 1997.
28. Ogata N, Jimenez G, Kawai H, Ogihara T. "Structure and thermal/mechanical properties of poly(L-lactide)–clay blend." *J. Polym. Sci., Part B: Polym Phys*; 35, 389–96, 1997.
29. Jeon HG, Jung HT, Lee SW, Hudson SD., "Morphology of polymer silicate nanocomposites. High density polyethylene and a nitrile." *Polym. Bull.*; 41, 107–13, 1998.
30. Kawasumi M, Hasegawa N, Usuki A, Okada A., "Nematic liquid crystal/clay mineral composites." *Mater. Sci. Engng. C*; 6, 135–43,1998.
31. Vaia RA, Giannelis EP., "Lattice of polymer melt intercalation in organically-modified layered silicates. *Macromolecules*; 30, 7990–9, 1997.
32. Wu J, Lerner M.M., "Structural, thermal, and electrical characterization of layered nanocomposites derived from sodium-montmorillonite and polyethers." *Chem. Mater.*; 5, 835–8, 1993.
33. Burnside S.D, Giannelis E.P., "Synthesis and properties of new poly (dimethylsiloxane) nanocomposites. *Chem. Mater.*; 7, 1597–600, 1995.
34. Yano K, Usuki A, Okada A. "Synthesis and properties of polyimide–clay hybrid films." *J. Polym. Sci., Part A: Polym Chem.*; 35, 2289–94, 1997.
35. Usuki A, Kawasumi M, Kojima Y, Okada A, Kurauchi T, Kamigaito O., "Swelling behavior of montmorillonite cation exchanged for α -amine acid by ϵ -caprolactam." *J. Mater. Res.*; 8, 1174–8, 1993.
36. Messersmith PB, Giannelis EP., "Polymer-layered silicate nanocomposites: in-situ intercalative polymerization of 1 - caprolactone in layered silicates." *Chem Mater*; 5, 1064–6, 1993.

37. Messersmith P.B, Giannelis E.P., "Synthesis and barrier properties of poly(1 -caprolactone)-layered silicate nanocomposites." *J. Polym. Sci., Part A: Polym. Chem.*; 33, 1047–57, 1995.
38. Chen T.K, Tien Y.I, Wei K.H., "Synthesis and characterization of novel segmented polyurethane/clay nanocomposite via poly(1 -caprolactone)/clay." *J. Polym. Sci., Part A: Polym. Chem.*; 37, 2225–33, 1999.
39. Okamoto M, Morita S, Taguchi H, Kim Y.H, Kotaka T, Tateyama H. "Synthesis and structure of smectic clay/ poly(methyl methacrylate) and clay polystyrene nanocomposites via in situ intercalative polymerization." *Polymer*; 41, 3887–90, 2000.
40. Okamoto M, Morita S, Kotaka T., "Dispersed structure and ionic conductivity of smectic clay/polymer nanocomposites." *Polymer*; 42, 2685–8, 2001.
41. Vaia R.A, Giannelis E.P., "Polymer melts intercalation in organically-modified layered silicates: model predictions and experiment." *Macromolecules*; 30, 8000–9, 1997.
42. Beyer F.L, Tan N.C.B, Dasgupta A, Galvin M.E., "Polymerlayered silicate nanocomposites from model surfactants." *Chem Mater*; 14, 2983–8, 2002.
43. Usuki A, Kato M, Okada A, Kurauchi T. "Synthesis of polypropylene–clay hybrid." *J. Appl. Polym. Sci.*; 63, 137–8, 1997.
44. Kawasumi M, Hasegawa N, Kato M, Usuki A, Okada A. "Preparation and mechanical properties of polypropylene–clay hybrids." *Macromolecules*; 30, 6333–8, 1997.
45. Hasegawa N, Kawasumi M, Kato M, Usuki A, Okada A., "Preparation and mechanical properties of polypropylene –clay hybrids using a maleic anhydride-modified polypropylene oligomer." *J. Appl. Polym. Sci.*; 67, 87–92, 1998.
46. Pantoustier N, Alexandre M, Degee P, Calberg C, Jerome R, Henrist C, Cloots R, Rulmont A, Dubois P., "Poly(1-caprolactone) layered silicate nanocomposites: effect of clay surface modifiers on the melt intercalation process." *e-Polymer*; 9,1–9, 2001.

47. Nam P.H, Maiti P, Okamoto M, Kotaka T, Hasegawa N, Usuki A., "A hierarchical structure and properties of intercalated polypropylene/clay nanocomposites." *Polymer*; 42, 9633–40, 2001.
48. Manias E., "A direct-blending approach for polypropylene/ clay nanocomposites enhances properties." *Mater. Res. Soc. Bull.*; 26, 862–3, 2001.
49. Zhu J, Morgan A.B, Lamelas F.J, Wilkie C.A., "Fire properties of polystyrene–clay nanocomposites." *Chem. Mater.*; 13, 3774–80, 2001.
50. Yano K, Usuki A, Okada A, Kurauchi T, Kamigaito O., "Synthesis and properties of polyimide–clay hybrid." *J. Polym. Sci., Part A: Polym Chem*; 31, 2493–8, 1993.
51. Nam P.H, Maiti P, Okamoto M, Kotaka T., "Foam processing and cellular structure of polypropylene/clay nanocomposites." *Proceeding Nanocomposites*, June 25–27, 2001, Chicago, Illinois, USA: ECM Publication; 2001.
52. Strawhecker K.E, Manias E., "Structure and properties of poly(vinyl alcohol)/NaS-montmorillonite nanocomposites." *Chem. Mater*; 12, 2943–9, 2000.
53. Pinnavaia T.J, Beall G.W, "Polymer-Clay Nanocomposites", John Wiley and Sons, England, 150-155, 2000.